UNIVERSIDADE FEDERAL DO PARANÁ

LUIS FELIPE LIMA POMPEO MARINHO

DESENVOLVIMENTO DE BOLHAS RETINIANAS EM CÃES COM ATROFIA PROGRESSIVA DE RETINA. AVALIAÇÃO DA CICATRIZAÇÃO, ESPESSURA E TRANSPARÊNCIA CORNEANA POR ULTRASSOM UBM APÓS REALIZAÇÃO DE CROSSLINKING EM CÃES COM ÚLCERAS PROFUNDAS E DEGRADADAS.

CURITIBA

2025

LUIS FELIPE LIMA POMPEO MARINHO

DESENVOLVIMENTO DE BOLHAS RETINIANAS EM CÃES COM ATROFIA PROGRESSIVA DE RETINA. AVALIAÇÃO DA CICATRIZAÇÃO, ESPESSURA E TRANSPARÊNCIA CORNEANA POR ULTRASSOM UBM APÓS REALIZAÇÃO DE CROSSLINKING EM CÃES COM ÚLCERAS PROFUNDAS E DEGRADADAS.

Tese apresentada ao Curso de Pós-Graduação em Ciências Veterinárias, Setor de Ciências Agrárias, da Universidade Federal do Paraná, como requisito parcial à obtenção do título de Doutor em Ciências Veterinárias.

Orientador: Prof. Dr. Fabiano Montiani-Ferreira

CURITIBA

2025

DADOS INTERNACIONAIS DE CATALOGAÇÃO NA PUBLICAÇÃO (CIP) UNIVERSIDADE FEDERAL DO PARANÁ
SISTEMA DE BIBLIOTECAS – BIBLIOTECA DE CIÊNCIAS AGRÁRIAS

Marinho, Luis Felipe Lima Pompeo
Desenvolvimento de bolhas retinianas em cães com atrofia progressiva de retina: avaliação da cicatrização, espessura e transparência corneana por Ultrassom UBN após realização de Crosslinking em cães com úlceras profundas e degradadas / Luis Felipe Lima Pompeo Marinho. – Curitiba, 2025.
1 recurso online: PDF.

Tese (Doutorado) – Universidade Federal do Paraná, Setor de Ciências Agrárias, Programa de Pós-Graduação em Ciências Veterinárias.
Orientador: Prof. Dr. Fabiano Montiani-Ferreira

1. Cães - Doenças. 2. Retina - Doenças. 3. Úlcera da córnea.
4. Oftalmologia veterinária. I. Montiani-Ferreira, Fabiano. II. Universidade Federal do Paraná. Programa de Pós-Graduação em Ciências Veterinárias. III. Título.

Bibliotecária: Elizabeth de Almeida Licke da Luz CRB-9/1434

TERMO DE APROVAÇÃO

Os membros da Banca Examinadora designada pelo Colegiado do Programa de Pós-Graduação CIÊNCIAS VETERINÁRIAS da Universidade Federal do Paraná foram convocados para realizar a arguição da tese de Doutorado de **LUIS FELIPE LIMA POMPEO MARINHO**, intitulada: **Desenvolvimento de bolhas retinianas em cães com atrofia progressiva de retina. Avaliação da cicatrização, espessura e transparência corneana por Ultrassom UBM após realização de Crosslinking em cães com úlceras profundas e degradadas.**, sob orientação do Prof. Dr. FABIANO MONTIANI FERREIRA, que após terem inquirido o aluno e realizada a avaliação do trabalho, são de parecer pela sua APROVAÇÃO no rito de defesa.

A outorga do título de doutor está sujeita à homologação pelo colegiado, ao atendimento de todas as indicações e correções solicitadas pela banca e ao pleno atendimento das demandas regimentais do Programa de Pós-Graduação.

CURITIBA, 06 de Agosto de 2025.

Assinatura Eletrônica
13/08/2025 16:59:51.0
FABIANO MONTIANI FERREIRA
Presidente da Banca Examinadora

Assinatura Eletrônica
06/08/2025 19:47:33.0
PETERSON TRICHES DORNBUSCH
Avaliador Interno (UNIVERSIDADE FEDERAL DO PARANÁ)

Assinatura Eletrônica
21/08/2025 12:38:04.0
PAULA STIEVEN HUNNING
Avaliador Externo (UNIVERSIDADE FEDERAL DO RIO GRANDE DO SUL)

Assinatura Eletrônica
07/08/2025 23:24:03.0
JUAN CARLOS DUQUE MORENO
Avaliador Interno (UNIVERSIDADE FEDERAL DO PARANÁ)

Assinatura Eletrônica
06/08/2025 14:42:09.0
ROGERIO RIBAS LANGE
Avaliador Interno (UNIVERSIDADE FEDERAL DO PARANÁ)

RESUMO

Objetivo: Integrar e comparar evidências clínicas e de imagem em dois domínios-chave da oftalmologia veterinária: (1) caracterização de descolamentos focais bolhosos da retina (bolhas) em diferentes formas geneticamente distintas de atrofia progressiva da retina (APR) e (2) avaliação da cicatrização da córnea, alterações paquimétricas e transparência após o tratamento com cromóforo fotoativado para ceratite-crosslinking da córnea (PACK-CXL) em úlceras corneanas infecciosas e degradativas ("derretimento"), que são particularmente prevalentes em raças braquicefálicas. Métodos: (1) Cães afetados por APR (cruzamentos de Whippet, Spitz Alemão e Papillon portadores de mutações no gene CNGB1) foram submetidos a oftalmoscopia indireta e tomografia de coerência óptica de domínio espectral (SD-OCT) para monitoramento longitudinal das bolhas retinianas. As sequências codificadoras e intrônicas flanqueadoras de BEST1 foram sequenciadas em pelo menos um cão afetado por raça, e um cão mutante para CNGB1 recebeu terapia de aumento gênico. (2) Vinte e quatro olhos com úlceras infecciosas ou degradativas foram tratados com PACK-CXL (riboflavina/UVA). A espessura da córnea foi medida usando paquimetria ultrassônica (UP) e biomicroscopia ultrassônica (UBM). A opacidade da córnea foi quantificada objetivamente a partir de imagens de UBM usando o ImageJ®. Quando disponíveis, os olhos contralaterais serviram como controles pareados. Resultados: (1) Bolhas retinianas foram achados precoces frequentes, precedendo o afinamento retiniano evidente e tornando-se menos evidentes à medida que a degeneração progredia; elas estavam ausentes em portadores heterozigotos. O sequenciamento de BEST1 não revelou variantes patogênicas. A amplificação gênica em um cão mutante para CNGB1 pareceu prevenir a formação de bolhas. (2) Após o PACK-CXL, todos os 24 olhos reepitelizaram em 30 dias. Nenhuma diferença estatisticamente significativa na espessura da córnea entre os olhos tratados e os controles foi detectada por ultrassonografia (UP), enquanto a biomicroscopia ultrassônica (UBM) revelou diferenças significativas. Comparando as modalidades, a diferença de espessura entre UP e UBM diferiu de zero em todos os subgrupos, indicando discordância sistemática dependente da modalidade. A análise quantitativa da opacidade mostrou opacidade significativamente maior nos olhos tratados do que nos controles contralaterais, tanto avaliando o estroma isoladamente quanto o estroma mais o epitélio. Conclusões: As bolhas retinianas representam um marcador clínico precoce e potencialmente modificável em múltiplas atrofias retinianas caninas e podem responder à terapia gênica. O PACK-CXL surge como um adjuvante promissor e custo-efetivo para o tratamento de úlceras infecciosas ou ulceradas. A ultrassonografia (UP) e a biomicroscopia ultrassônica (UBM) são ferramentas complementares para o monitoramento da espessura da córnea, apesar de diferenças sistemáticas, e a UBM permite a quantificação objetiva da opacidade por meio do ImageJ®. Mais estudos randomizados e controlados são necessários para ampliar a base de evidências e refinar as indicações clínicas.

Palavras-chave: atrofia progressiva da retina; bolhas retinianas; CNGB1; BEST1; PACK-CXL; riboflavina/UVA; paquimetria ultrassônica; biomicroscopia ultrassônica; opacidade da córnea; SD-OCT; oftalmologia canina.

ABSTRACT

Objective: To integrate and compare clinical and imaging evidence in two key domains of veterinary ophthalmology: (1) characterization of focal bullous retinal detachments (bullae) across genetically distinct forms of progressive retinal atrophy (PRA), and (2) assessment of corneal healing, pachymetric changes, and transparency following photoactivated chromophore for keratitis-corneal cross-linking (PACK-CXL) in infectious, degradative ("melting") corneal ulcers, which are particularly prevalent in brachycephalic breeds. Methods: (1) PRA-affected dogs (Whippets, German Spitzes, and Papillon crosses carrying CNGB1 mutations) underwent indirect ophthalmoscopy and spectral-domain optical coherence tomography (SD-OCT) for longitudinal monitoring of retinal bullae. The coding and flanking intronic sequences of BEST1 were sequenced in at least one affected dog per breed, and one CNGB1-mutant dog received gene-augmentation therapy. (2) Twenty-four eyes with infectious or degradative ulcers were treated with PACK-CXL (riboflavin/UVA). Corneal thickness was measured using ultrasonic pachymetry (UP) and ultrasound biomicroscopy (UBM). Corneal opacity was objectively quantified from UBM images using ImageJ®. When available, contralateral eyes served as paired controls. Results: (1) Retinal bullae were frequent early findings, preceding overt retinal thinning and becoming less evident as degeneration progressed; they were absent in heterozygous carriers. BEST1 sequencing revealed no pathogenic variants. Gene augmentation in a CNGB1-mutant dog appeared to prevent bulla formation. (2) After PACK-CXL, all 24 eyes re-epithelialized within 30 days. No statistically significant difference in corneal thickness between treated and control eyes was detected by UP, whereas UBM revealed significant differences. Comparing modalities, the UP-UBM thickness delta differed from zero across all subgroups, indicating systematic, modality-dependent disagreement. Quantitative opacity analysis showed significantly greater opacity in treated eyes than in contralateral controls, whether assessing the stroma alone or stroma plus epithelium. Conclusions: Retinal bullae represent an early and potentially modifiable clinical marker in multiple canine PRAs and may respond to gene therapy. PACK-CXL emerges as a promising and cost-effective adjunct for the management of infectious or melting ulcers. UP and UBM are complementary tools for monitoring corneal thickness despite systematic differences, and UBM allows objective opac quantification via ImageJ®. Further randomized, controlled studies are warranted to expand the evidence base and refine clinical indications.

Keywords: progressive retinal atrophy; retinal bullae; CNGB1; BEST1; PACK-CXL; riboflavin/UVA; ultrasonic pachymetry; ultrasound biomicroscopy; corneal opacity; SD-OCT; canine ophthalmology.

DEDICATÓRIA

Dedico aos meus pais, Valdir Marinho e Rose Pompeo, pela educação, e à minha filha, Clara Filipa, que me ensinou o amor incondicional.

AGRADECIMENTOS

Agradeço ao Professor Dr. Fabiano Montiani-Ferreira, Professor Dr. Simon Petersen-Jones, aos membros das bancas examinadoras, corpo docente e coordenação da Pós-Graduação da Universidade Federal do Paraná e Michigan State University pela oportunidade e aprendizado.

“Ciência é como o tempo”

Ciência é como o tempo em que só o presente instante existe, o passado se transforma e o futuro nunca chega. São invenções da humanidade representadas pela contagem da nossa própria destruição e resultam de uma sucessão de descobertas que juntos formam os periódicos que são frutos das transformações instantâneas onde o espaço desaparece e nos tornamos simultâneos.

Ciência é como o tempo a ponto de nos impedir de viver ritmos biológicos naturais gerando ansiedade e infelicidade por ser tão mutável. Nossa mente sempre questiona e com o tempo criamos a ciência que é o êxtase criativo dos seres que tem tempo num mundo onde quem trabalha não tem tempo para pensar.

Ciência e o tempo marcam a revolução da longevidade e estão reprogramando o *software* da vida e criando a simbiose entre homens e máquinas em que o resultado será a trans humanidade e nos permitirão alcançar a divindade com a decodificação genética assim como antigamente encontrar a espiritualidade dos deuses com a religião.

Portanto, a ciência é a infinitude do tempo.

(Desconhecido, tempo infinito)

INDEX

1 PRESENTATION

Progressive retinal atrophy (PRA) is the commonest category of inherited retinal degeneration in dogs. The term describes a group of inherited degenerative disorders of the retina with shared clinical signs that result in vision impairment and blindness. PRA has been identified in more than one hundred breeds of dogs (Petersen- Jones SM, Komaromy AM, 2015; Petersen Jones SM, Mowat FM, 2021). The typical clinical signs of PRA include a loss of night vision and on funduscopic examination indications of progressive retinal thinning (eg, tapetal hyperreflectivity) and accompanying retinal vascular attenuation (Winkler PA et al., 2013).

A form of PRA reported in Whippets by Somma et al. (2007) has been associated with the formation of multiple retinal bullae, a change that had not been previously reported in dogs with PRA. Further studies are required to understand the additional factors that lead to bullae formation and why it occurs in these three forms of PRA. A better understanding of this finding may support the development of future translational approaches, including retinal gene therapy, aimed at treating inherited diseases and restoring vision in millions of animals and humans worldwide.

The advantages of the dog model include the similarity of eye size to that of human, enabling identical approaches to administer gene therapy, and the presence of a region of higher photoreceptor density, the *area centralis.* The spontaneous dog models often show a very similar disease phenotype to human patients, making them very useful for investigating disease mechanism and testing therapy (Petersen- Jones SM, Komaromy AM, 2015; Petersen Jones SM, Mowat FM, 2021).

In chapter 1, we provide further details of bullae formation in PRA- affected Whippets and report that retinal bullae are a feature of two other forms of PRA. In addition, in one of those forms of PRA underwent retinal gene augmentation therapy and we show preliminary data suggesting that gene therapy can prevent bullae formation.

In conclusion, veterinarians should be aware that retinal bullae can develop in some forms of PRA and occur prior to retinal thinning and that they are no longer apparent once retinal degeneration is established. The retina in the affected region appears to degenerate more rapidly than in the adjacent regions not affected by bullae being Optical Coherence Tomography (SD- OCT) a sensitive tool for detecting these bullae.

This study was published by the Veterinary Ophthalmology on October 28, 2021, titled " Development of retinal bullae in dogs with progressive retinal atrophy" (ANNEX 1).

Ulcerative keratitis is one of the major ophthalmic diseases in dogs and is a potentially sight-threatening condition of the cornea often presenting as an ophthalmic emergency requiring prompt medical attention to prevent keratomalacia, melting keratitis, other complications and vision loss (Marcato PS., 2015; Jones DB., 1981).

Corneal melting results from the enzymatic degradation of stromal collagen by matrix metalloproteinases (MMPs), which are released endogenously and exogenously and an imbalance

between these proteolytic enzymes and the proteinase inhibitors present in the cornea and the precorneal tear film often caused by a secondary bacterial or fungal corneal infection resulting in a typical appearance of a gelatinous collagenolysis. Progression of both keratomalacia and infectious keratitis may result in significant corneal scarring and corneal perforation, ultimately threatening vision and loss of the globe (Ollivier FJ et al., 2003; Ollivier FJ et al.,2007; Fini ME, Girard MT, 1990; Perez VL et al., 2002; Marcon AS et al., 2003; Geerling G et al., 1999).

Treatment of corneal ulcers aims to eradicate the underlying cause and reduce inflammation and the ocular immune response in order to preserve the transparency of the tissue as much as possible. Intensive treatment with topical antimicrobials to treat a potential infection and Anti-collagenase therapy is initiated to try to mitigate collagen loss and retain as much corneal tissue as possible to stop progression of the melting process.

In case of clinical treatment failure or other ocular co-morbidities may require additional treatments such as surgery to prevent corneal scarring and vision loss including Corneal Crosslinking (CXL) (Spiess BM et al., 2013).

The CXL is a photodynamic therapy which consists in the administration of an ophthalmic solution enriched with riboflavin (vitamin B2) followed by irradiation of the cornea with ultraviolet A light (UV-A) (Maier Philip., et al., 2019; Moghadam., et al., 2019) riboflavin (vitamin B2) acts as photosensitizer when exposed to UV-A light with a wavelength of 370 nm creating new chemical bonds in the stroma matrix via photopolymerization.

CXL increases the biochemical strength and stabilizes the cornea by forming new crosslinks in the corneal stroma between collagen fibers and proteoglycan core proteins resulting in an increased collagen packing density, more resistant to enzymatic digestion, modulation of melting and bacterial colonization through steric hindrance. Additionally, the free radicals induced by CXL directly damage and destroy microorganisms and lead to apoptosis of cells in the irradiation area (Spoerl E et al., 1998; Spoerl E et al., 2004; Wollensak G et al., 2004).

The use of CXL as an adjunctive therapy for the treatment of melting Keratitis may become its major indication in veterinary medicine and the consisted phototherapy protocol of 30mW/cm² UV-A power irradiance for 3 minutes with a total emitted energy dose of 5.4 J/cm² was validated in the laboratory for exclusive use in veterinary medicine (VET-CXL® protocol) (Razmjoo et al., 2017; Famose, 2016; Huang Jinrong et al., 2018).

In chapter 2, we studied the application of this promising and revolutionary therapy in dogs with serious ophthalmic ulcers conditions presenting melting using the gold standard Riboflavin and equipment in the veterinary market (PXL VELVET 345, Peschke Meditrade GmbH, Switzerland). The objective of this study was to evaluate the healing, compare the corneal thickness of treated and non-treated eyes using ultrasonic pachymetry and UBM ultrasound as well as evaluation of the corneal transparency using the UBM images and software ImageJ® after PACK-CXL in infected and degraded ulcers in dogs.

2 DEVELOPMENT OF RETINAL BULLAE IN DOGS WITH PROGRESSIVE RETINAL ATROPHY

ABSTRACT

Objective: To report the development of focal bullous retinal detachments (bullae) in dogs with different forms of progressive retinal atrophy (PRA). Procedures: Dogs with three distinct forms of PRA (PRA- affected Whippets, German Spitzes and CNGB1- mutant Papillon crosses) were examined by indirect ophthalmoscopy and spectral domain optical coherence tomography (SD-OCT). Retinal bullae were monitored over time. One CNGB1- mutant dog was treated with gene augmentation therapy. The canine BEST1 gene coding region and flanking intronic sequence was sequenced in at least one affected dog of each breed. Results: Multiple focal bullous retinal detachments (bullae) were identified in PRA- affected dogs of all three types. They developed in 4 of 5 PRA- affected Whippets, 3 of 8 PRA- affected Germans Spitzes and 15 of 20 CNGB1- mutant dogs. The bullae appeared prior to marked retinal degeneration and became less apparent as retinal degeneration progressed. Bullae were not seen in any heterozygous animals of any of the types of PRA. Screening of the coding region and flanking intronic regions of the canine BEST1 gene failed to reveal any associated pathogenic variants. Retinal gene augmentation therapy in one of the CNGB1- mutant dogs appeared to prevent formation of bullae. Conclusions: Retinal bullae were identified in dogs with three distinct forms of progressive retinal atrophy. The lesions develop prior to retinal thinning. This clinical change should be monitored for in dogs with PRA.

Keywords: BEST1, bullae, bullous retinal detachment, CNGB1, dog, progressive retinal atrophy

2.1 INTRODUCTION

Progressive retinal atrophy (PRA) is the commonest category of inherited retinal degeneration in dogs. The term describes a group of inherited degenerative disorders of the retina with shared clinical signs that result in vision impairment and blindness. PRA has been identified in more than one hundred breeds of dogs (Petersen- Jones SM, Komaromy AM, 2015; Petersen Jones SM, Mowat FM, 2021). It is most commonly a rod- led degeneration (rod- cone dystrophy), with secondary and slower loss of cones that leads in many instances to complete blindness. The molecular genetic basis of the condition has been investigated in many dog breeds revealing the genetic heterogeneity of the condition, a feature shared with the analogous human condition, retinitis pigmentosa. In some forms of PRA studies have shown that cones are either involved prior to, or at the same time as rods, such phenotypes are classified as cone- rod dystrophies (Ropstad EO, Bjerkas E et al., 2007; Goldstein O et al., 2010). However, the funduscopic changes indicating a bilateral progressive retinal thinning are similar to those of the rod- cone dystrophies.

The typical clinical signs of PRA include a loss of night vision and on funduscopic examination indications of progressive retinal thinning (eg, tapetal hyperreflectivity) and accompanying retinal vascular attenuation. In some forms of PRA, tapetal hyporeflectivity may be an early change (Winkler PA et al., 2013), perhaps indicating that prior to the death of photoreceptors and resulting retinal thinning, alterations are occurring that result in absorption of more of the examination light. Some forms of PRA have changes specific to that particular form;

for example, dominant PRA due to a rhodopsin mutation renders the retina of affected dogs very sensitive to light damage. This can lead to patchy degeneration brought on by environmental light exposure (Sudharsan R. et al., 2017). A form of PRA reported in Whippets by Somma et al. (2007) has been associated with the formation of multiple retinal bullae, a change that had not been previously reported in dogs with PRA. In addition, Dufour et al. (2020) recently reported that they occasionally observe transient retinal separation in dogs with X- linked PRA type 2 which is due to a mutation in the RPGR (Retinitis Pigmentosa GTPase Regulator) gene.

In this study, the authors provide further details of bullae formation in PRA- affected Whippets and report that retinal bullae are a feature of two other forms of PRA. In addition, in one of those forms of PRA we show preliminary data suggesting that gene therapy can prevent bullae formation.

2.2 MATERIALS AND METHODS

2.2.1 Animals

Procedures were conducted according to the ARVO statement for Use of Animals in Ophthalmic and Vision Research. The study at Michigan State University was approved by the Institutional Animal Care and Use Committee. Studies in Brazil were approved by the Animal Use Ethics Committee of the Federal University of Paraná.

Three groups of dogs with three different forms of autosomal recessive PRA were included. Only dogs examined at early disease stages were included. Heterozygous littermates were also examined for the two groups maintained in a colony. The first group consisted of 5 PRA- affected Whippets (4 males and one female) and 3 males heterozygous for PRA from a colony of Whippets established at Michigan State University derived from the previously reported PRA- affected Whippets (Somma et al., 2007; Marinho LLP et al., 2020). These dogs were monitored from 3 months up to at least 18 months of age. The second group consisted of 8 PRA- affected (6 male and 2 females) privately- owned German Spitzes aged 3– 12 months diagnosed and examined at the Veterinary Teaching Hospital of the Federal University of Paraná (Brazil). The final group consisted of 20 Papillon beagle crosses (11 males, 9 females) homozygous for a previously described mutation in rod cyclic nucleotide gated channel subunit beta 1 (CNGB1) (Winkler PA et al., 2013) followed from 3 to at least 18 months of age. One of these dogs underwent retinal gene augmentation therapy as previously reported. Six dogs heterozygous for the CNGB1 mutation (1 male, 5 females) were also examined. The Whippet and Papillon crosses were housed in the same facility under a 12/12 h light cycle and fed the same commercial dog food.

2.2.2 Eye examination and fundus photographs

For examination and spectral domain optical coherence tomography pupils were dilated with tropicamide (1% Tropicamide, Akorn Inc., or Alcon Laboratórios do Brasil). Ophthalmic examination included slit- lamp biomicroscopy (Kowa® SL- 17, Kowa American Corporation or Hawk Eye; Dioptrix), indirect ophthalmoscopy (Keller Vantage Plus wireless LED, Keeler Instruments and Heine Omega 200; Heine Instruments) and fundus color images were collected with a RetCam II (Clarity Medical Systems, Inc) or a ClearView Optical Imaging System (Optibrand).

2.2.3 Spectral domain optical coherence tomography (SD- OCT)

Retinal imaging was performed with dogs under general anesthesia. Briefly, the dogs were pre- medicated with subcutaneous or intramuscular acepromazine (0.02– 0.1 mg/Kg; Aceprojet, Henry Schein Animal Health or Acepran, 0.2%— Vetnil) and in some cases with buprenorphine (0.01– 0.03 mg/kg; Reckitt Benckiser Company). Anesthesia was induced with intravenous propofol (4– 6 mg/kg; PropoFlo, Zoetis or Propovan 1%, Cristália), and maintained on 1.5%– 3% Isoflurane (Isothesia Inc, Henry Schein Animal Health). Eyes were positioned in primary gaze using conjunctival stay sutures (4– 0 or 6– 0 silk, Ethicon, LLC, Johnson & Johnson Company). Imaging was performed using a combined confocal scanning laser ophthalmoscopy (cSLO) and spectral domain optical coherence tomography (SD- OCT) (Spectralis HRA/OCT, Heidelberg Engineering). Infrared (IR) and autofluorescence (AF) cSLO images of the fundus were acquired using a 55° lens. Horizontal and vertical SD- OCT single line scans as well as raster volume scans from the areas with bullae and from the rest of the retina were obtained using a 30° lens.

2.2.4 Screening canine best1 gene for variant

Canine multifocal retinopathy (CMR) is associated with retinal bullae formation and is due to homozygous mutations in the BEST1 gene (Guziewicz KE et al., 2007; Zangerl B et al., 2010) To screen for the unlikely possibility that a BEST1 mutation was segregating in the PRA- affected dog pedigrees the entire coding region (including parts of the flanking introns) were Sanger sequenced in two affected Whippets and one CNGB1- mutant dog. The sequence for PRA- affected German Spitz was obtained from whole genome sequencing of 2 PRA- affected dogs. For Sanger sequencing blood DNA was extracted using standard protocols and polymerase chain reaction used to amplify the coding region and intronic regions flanking exons of the BEST1 gene (see Table S1 for the PCR primers used). Amplicons were submitted for Sanger sequencing. The resulting DNA sequence was aligned to the canine reference sequence using Canfam 3.1 and screened for any polymorphisms. Whole genome sequencing was performed as previous described (Winkler PA et al., 2013). Aligned sequence files were viewed using Integrated Genomics Viewer (version 2.4.9) and screened for variants from the Canfam 3.1 genome in the coding exons and flanking intronic regions of BEST1.

2.2.5 Gene augmentation therapy

An adeno-associated viral construct (serotype 5) packaged with CNGB1 cDNA was delivered by two subretinal injections of about 200 µl of a titer of 5 x 1011 vg/ml. Procedures have been previously described (Petersen- Jones SM et al., 2018)

2.3 RESULTS

2.3.1 Fundus imaging

Multiple retinal bullae were detected in dogs with all three types of PRA. The age they were first identified varied between breeds being as early as 3 months of age in the Whippets to about 6 months of age in the German Spitz. In addition, the localization, number and size of the bullae differed between the groups (Figures 1- 3). In all three breeds the subretinal fluid appeared to be clear on indirect ophthalmoscopy and color fundus imaging. On cSLO IR imaging the bullae were clearly visible in the tapetal fundus. On AF imaging bullae within the non- tapetal fundus showed hyperfluorescence. SD- OCT imaging confirmed that the lesions were focal bullous retinal detachments and the subretinal fluid was hyporeflective. SD- OCT was found to be a more sensitive method for detecting the presence of bullae, particularly those that were relatively flat detachments and those that were in the non- tapetal area.

Four of the 5 PRA- affected Whippets (2 males and 2 females) developed retinal bullae localized to the central tapetal fundus (Figure 1), but there were fewer bullae per eye compared to the other 2 groups. Bullae were detected from 3 months of age and were up to 1210 µm in diameter (Figure 1). They were first detectable by SD- OCT but most became large enough to be seen by indirect ophthalmoscopy and RetCam photography. Figure 4 shows serial SD- OCT examinations of the large bullae in a male PRA- affected Whippet. As the photoreceptor degeneration became apparent (ie, thinning of the photoreceptor layer became apparent on SD- OCT examination) the bullae tended to flatten, and the outer retina of the detached region degenerated more rapidly than the surrounding attached retina which can be clearly seen in the cross- sectional retinal images at 12 and 18 months ages (Figure 4). None of PRA carrier Whippets had bullae detected.

Three of the 8 PRA- affected German Spitz dogs developed multiple bullae (from 40 to 90 per eye) involving the whole tapetal area, with a tendency to be more concentrated near the dorsal blood vessels. Bullae diameter was always small, from one fourth to one sixth of the optic disk diameter (Figure 2). The precise age at development is not known but at 3 months of age bullae were not detected but when examined at 6 months of age they could be detected. Seven of the 8 PRA- affected German Spitz dogs were examined by SD- OCT as well as indirect ophthalmoscopy. One dog was only examined by indirect ophthalmoscopy and no bullae were detected in this animal.

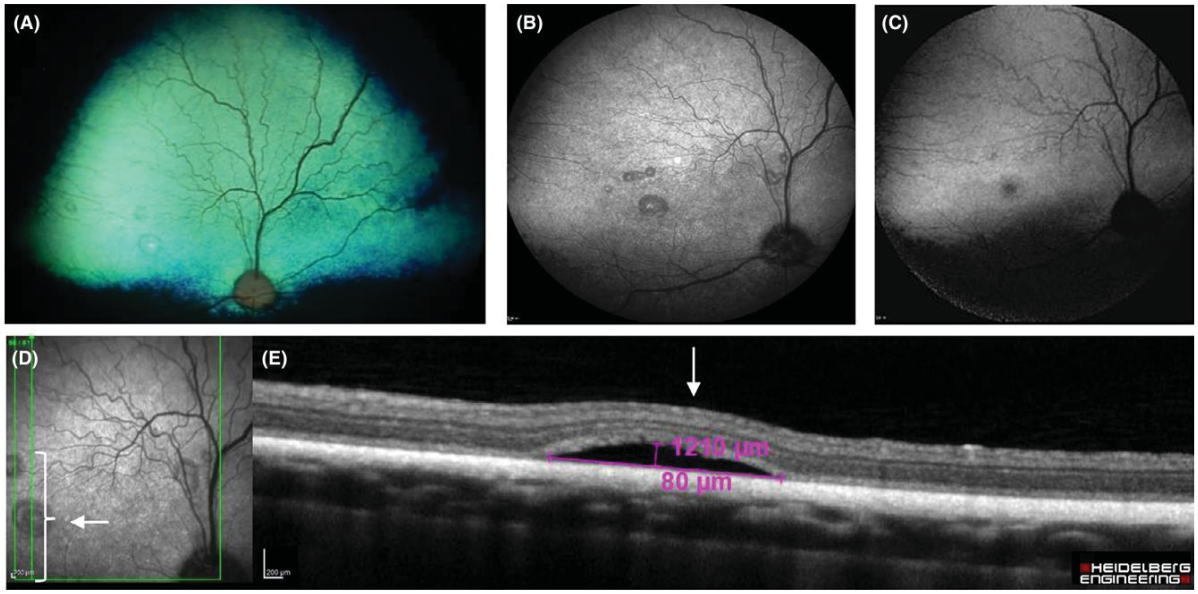

FIGURE 1. RETINAL BULLAE IN A PRA- AFFECTED WHIPPET. (A) WIDE- ANGLE COLOR FUNDUS IMAGE OF THE RIGHT EYE OF A 6- MONTH- OLD MALE WHIPPET SHOWING 1 LARGE BULLAE IN THE AREA CENTRALIS REGION AND SEVERAL SMALLER BULLAE. (B) CSLO INFRARED AND (C) AUTOFLUORESCENT IMAGE OF THE SAME DOG. (D) IR IMAGE, THE SITE OF THE MAGNIFIED SD- OCT IMAGE IN (E) IS INDICATED BY THE WHITE BRACKET. (E) SD- OCT HIGH RESOLUTION CROSS- SECTION IMAGE ACROSS THE BULLA IN THE AREA CENTRALIS REGION INDICATED IN D. IN PURPLE ARE THE MEASUREMENTS OF THE WIDTH AND HEIGHT OF THE BULLAE

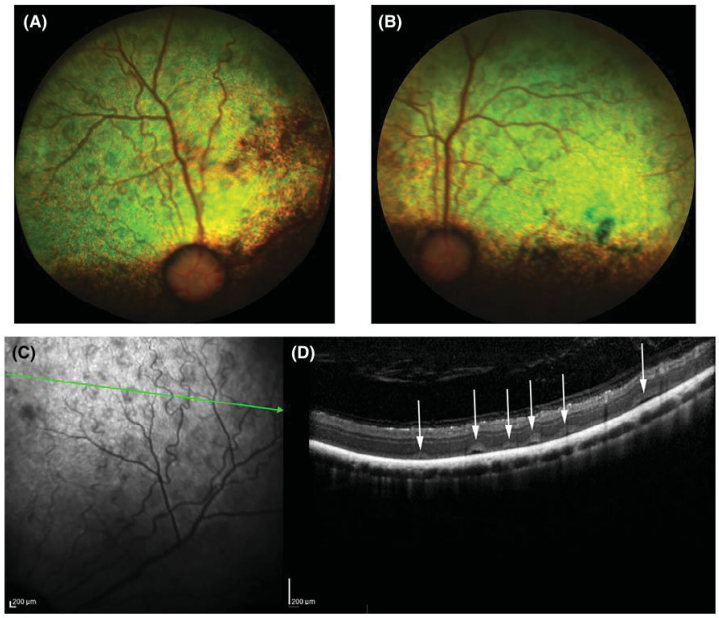

FIGURE 2. MULTIPLE BULLAE IN A PRA- AFFECTED GERMAN SPITZ DOG. (A AND B) ARE RIGHT AND LEFT EYES OF THE SAME FEMALE DOG AT 7 MONTHS OF AGE. (C) IS A CSLO INFRARED FUNDUS IMAGE OF THE RIGHT EYE INDICATING THE POSITION OF THE SD- OCT SCAN SHOWN IN (D). (D) MULTIPLE BULLAE ARE PRESENT ACROSS THE RETINAL CROSS- SECTIONAL SD- OCT IMAGE (INDICATED BY WHITE ARROWS)

Bullae were identified in 15 of the 20 CNGB1- mutant dogs. They varied between individual animals in size, but they tended to be numerous and first detected in the peripheral tapetal and non- tapetal fundi, before developing in the more central tapetal regions (Figure 3). They appeared to become larger in the periphery with the largest measured reaching 3800 µm in

diameter. As with the German Spitz the lesions were not present at the initial examinations of 2 – 3 months of age but appeared from about 4 months of age. They became more obvious at between 6 and 9 months of age then appeared to decrease from about 12−15 months of age. For 6 of the 15 with bullae these were detected by SD- OCT but were not apparent in the RetCam images and not noted on indirect ophthalmoscopy. The 5 CNGB1- mutant dogs in which bullae were not detected SD- OCT was not performed and they were only examined by indirect ophthalmoscopy and RetCam imaging. Bullae were not detected in any of the dogs heterozygous for the CNGB1 mutation.

The CNGB1- mutant dog that had undergone gene augmentation therapy did not develop bullae in the treated retinal regions but did develop multiple bullae in the sur rounding untreated retina (Figure 5).

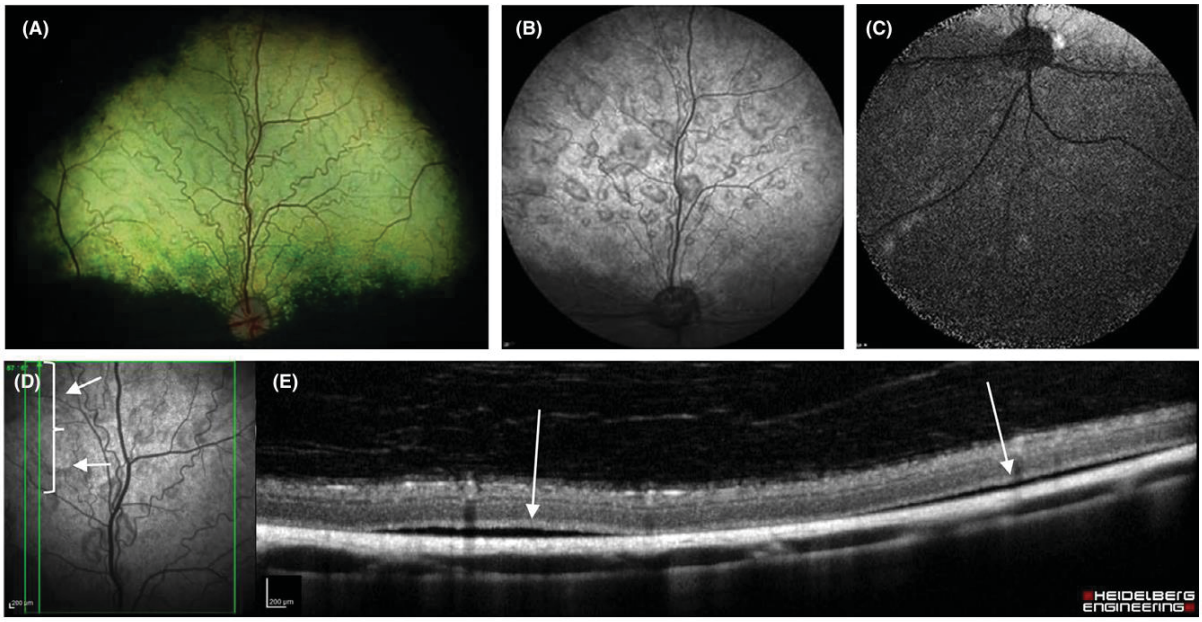

FIGURE 3. MULTIPLE BULLAE IN A HOMOZYGOUS CNGB1- MUTANT DOG (PAPILLON DERIVED). (A) WIDE-ANGLE FUNDUS COLOR IMAGE SHOWING PRESENCE OF MULTIPLE BULLAE ACROSS THE TAPETAL FUNDUS. (B) A CSLO INFRARED IMAGE OF THE TAPETAL REGION SHOWING THE MULTIPLE BULLAE. (C) A CSLO AUTOFLUORESCENT IMAGE OF THE NON- TAPETAL FUNDUS. BULLAE SHOW AS HYPERFLUORESCENT FOCAL REGIONS. (D) IR IMAGE THE SITE OF THE MAGNIFIED SD- OCT IMAGE IN (E) IS INDICATED BY THE WHITE BRACKET. (E) SD- OCT IMAGE ACROSS THE BULLA IN THE CENTRAL RETINA INDICATED IN (D). WHITE ARROWS INDICATE THE POSITION OF THE BULLAE IN (D AND E)

2.3.2 Sequence of exons and adjacent portions of the introns of Best1

Sequencing of the exons and flanking intronic regions of BEST1 in dogs of each breed revealed the presence of SNPs in the coding regions of exons 2, 4, 7 and 8 (Table S2). In each case these were synonymous variants which were previously recorded in the canine SNP database.

2.4 DISCUSSION

Progressive retinal atrophy in dogs has been recognized since the 1900s (Magnusson H, 1911). Today it is known that it is a genetically heterogeneous condition that varies between forms in mode of inheritance, age of onset and rate of progression (for a recent review of PRA see Petersen- Jones and Mowat 2021). The different forms of PRA share clinical features including a progressive photoreceptor loss leading to retinal thinning, retinal vascular attenuation and optic nerve head atrophy. The precise molecular mechanism under lying different genetic forms of PRA may differ and can include mechanisms such as failure of phototransduction leading to accumulation of cyclic GMP in photoreceptors (eg, in PDE6B and PDE6A mutations (Petersen-Jones et al., 2018, Aguirre GD et al., 1978).

We recently described a new form of PRA in Whippets in which retinal bullae formation occurred prior to retinal thinning (Somma AT et al., ,2017). There was also an absence of the ERG b- wave suggesting impaired photoreceptor to bipolar cell synaptic transmission (Marinho LLP et al., 2019). In the current study 4 of the 5 PRA- affected Whippets examined were identified to have bullae formation. Here we also report retinal bullae formation prior to retinal degeneration in two additional groups of dogs with two distinct forms of PRA; German Spitz with an early- onset autosomal recessive form of PRA and in dogs with PRA due to a mutation in CNGB1 that we have previously identified and characterized (*Winkler PA et al., 2013). In PRA- affected German Spitz 3 out of 8 of the examined dogs (prior to 12 months of age) and in CNGB1- mutant dogs 15 of 20 dogs examined were found to develop bullae. Bullae were not identified in any of the heterozygotes for the Whippet form of PRA nor heterozygotes for CNGB1- PRA. This strongly suggests that the presence of diseased photoreceptors prior to extensive cell death is necessary for the formation of bullae.

The bullae represent focal small bullous retinal detachments characterized by subretinal fluid accumulation. While many of the lesions could be seen by indirect ophthalmoscopy, SD- OCT was a more sensitive method to detect small, flatter detachments and in particular those in the non-tapetal fundus. In dogs where the lesions were monitored over time, the detached retinal region tended to degenerate more rapidly than the adjacent attached region (see Figure 4). This is most likely because of the additional deleterious effect of separation of the diseased photoreceptors from the supporting RPE.

There were some differences in the bullae between the three breeds. The Whippets tended to have fewer bullae compared to PRA- affected German Spitz and the CNGB1- mutant dogs. Retinal gene therapy in one CNGB1 dog seemed to prevent bullae formation just in the treated retinal regions. The therapy restored normal retinal function and preserved structure (data not shown) suggesting that the presence of abnormal and degenerating photoreceptors was necessary for the formation of the bullae.

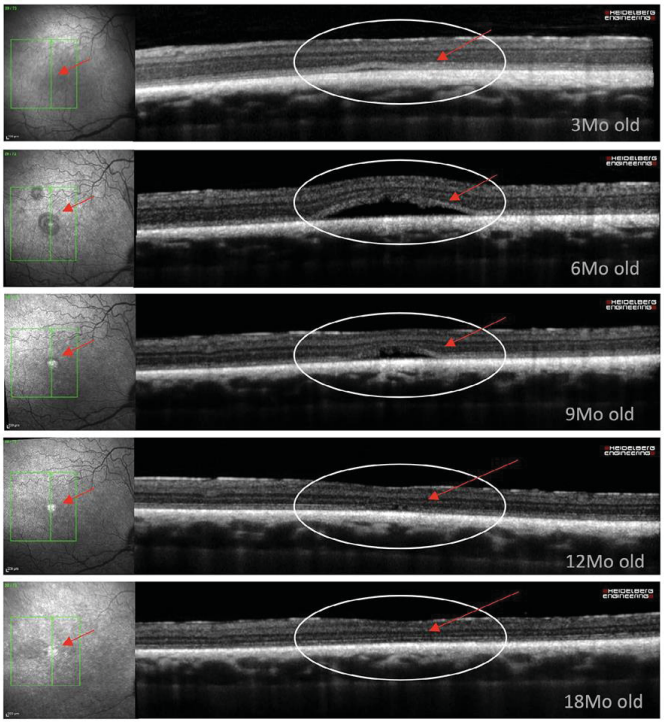

FIGURE 4 PROGRESSION OF THE RETINAL BULLA IN THE RIGHT EYE OF THE MALE PRA- AFFECTED WHIPPET SHOWN IN FIGURE 1. THE SAME REGION IS IMAGED STARTING AT 3 MONTHS OF AGE IN THE TOP IMAGE WHERE A SMALL BULLA IS PRESENT. NOTE THE EXPANSION OF THE BULLA BY 6 MONTHS OF AGE AFTER WHICH IT DECREASES IN SIZE. OUTER RETINAL THINNING IS APPARENT AT THE 12 AND 18 MONTH AGES. NOTE THAT THERE IS MORE SEVERE DEGENERATION IN THE REGION OF THE PREVIOUS BULLA. RED ARROWS INDICATE SAME REGION IN ALL IMAGES

The development of retinal bullae in dogs with 3 genetically distinct forms of PRA suggest that their formation is not specific to the PRA- causing gene mutation. The causal mutations in Whippets and German Spitz will be the subject of separate publications and are not in genes related to CNGB1 which is mutated in the Papillon derived dogs in this study. They are all photoreceptor specific genes and not expressed in RPE. There is an additional previous report of bullae formation in dogs with X- linked PRA type 2 (Dufour VL et al., 2020). Retinal bullae formation has also been reported by three independent groups in dogs with sudden acquired retinal degeneration syndrome (SARDS) (Osinchuk SC et al., 2019; Oh A et al., 2019; Grozdanic SD et al., 2019). As noted in the current study, the authors reporting retinal bullae formation in dogs with SARDS found SD- OCT a more sensitive tool to detect the presence of bullae. The development of bullae formation in several forms of PRA with different disease mechanisms and also in dogs with a non- inherited cause of photoreceptor degeneration suggests active photoreceptor degeneration is the common factor.

There are several possible mechanisms for the formation of subretinal fluid. These include disruption of the normal pump mechanism of the RPE or a loss of the integrity of the Blood Retinal Barrier (BRB). The RPE actively transports fluid out of the subretinal space, while keeping K+ and lactate levels in this compartment tightly controlled. This function of the RPE maintains a negative hydrostatic pressure, essential for the adhesion between RPE and photoreceptors; failure of this transport system leads to retinal edema and retinal detachment (Amer R et al., 2017). Bestrophin, encoded by the BEST1 gene, plays an important role in this process (for a review see) (Guziewicz KE et al., 2017).

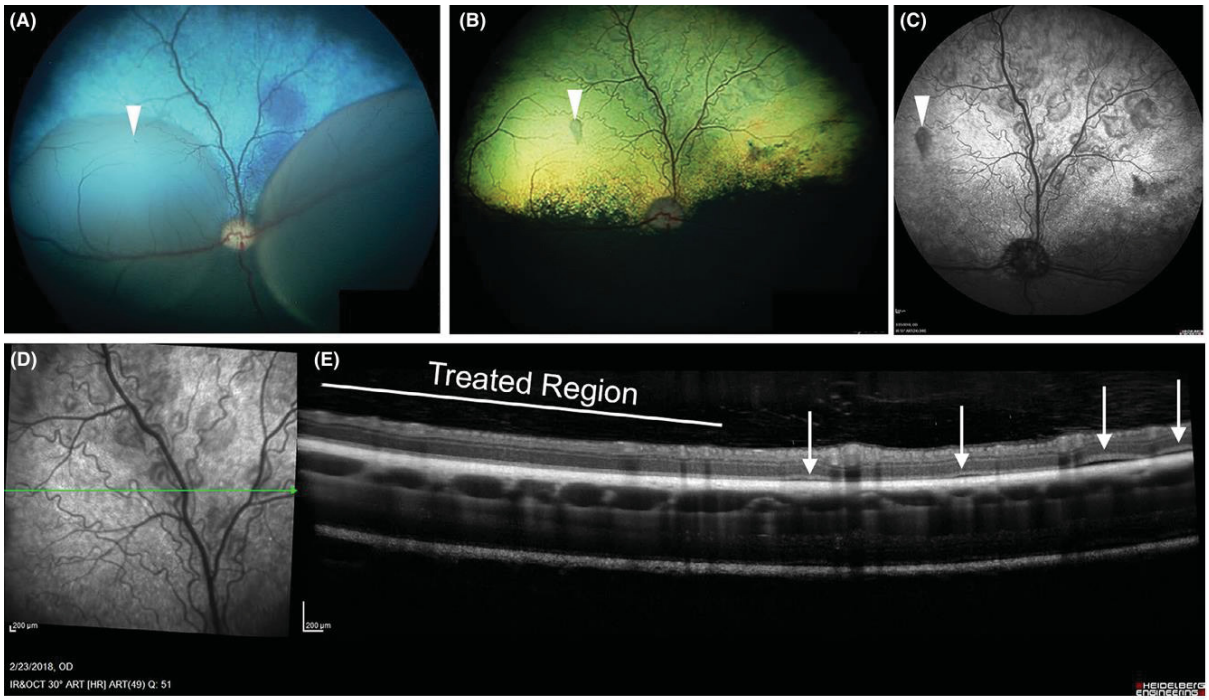

FIGURE 5 RETINAL GENE AUGMENTATION THERAPY IN A HOMOZYGOUS CNGB1- MUTANT DOG APPEARS TO PROTECT AGAINST RETINAL BULLAE FORMATION. (A) WIDE- ANGLE FUNDUS COLOR PHOTOGRAPH TAKEN IMMEDIATELY AFTER SUBRETINAL INJECTION OF AN AAV VECTOR DELIVERING A NORMAL COPY OF THE CDNA FOR CNGB1. TWO SEPARATE INJECTION BLEBS HAVE BEEN CREATED – DOG WAS 3 MONTHS OF AGE. THE RETINOTOMY SITE FOR ONE BLEB IS INDICATED BY A WHITE ARROWHEAD. (B) THE SAME EYE AS IN A 6 MONTHS POST THERAPY. NOTE THAT THERE ARE NO BULLAE IN THE REGION OF EITHER TREATMENT BLEB (ALSO NOTE THE SLIGHT CHANGE IN TAPETAL COLOR IN THE TREATED AREAS). THE NON- TREATED REGION HAS DEVELOPED MULTIPLE BULLAE. THE ARROWHEAD INDICATES THE SCAR FROM THE INJECTION RETINOTOMY. (C) CSLO INFRARED IMAGE SHOWING THE LACK OF BULLAE IN THE REGION OF THE GENE AUGMENTATION THERAPY TREATMENT. (D) A CSLO INFRARED IMAGE WITH A GREEN LINE INDICATING THE POSITION OF THE SD- OCT CROSS- SECTIONAL IMAGE IN (E). (E) SD- OCT ACROSS THE TREATED/UNTREATED RETINAL REGION. THE TREATED REGION IS INDICATED WITH THE WHITE LINE. THE PRESENCE OF BULLAE IN THE UNTREATED REGION IS SHOWN BY THE ARROWS

The BRB (inner/outer) plays an important role in the homeostatic regulation of the retinal microenvironment by controlling fluid and molecular movement between the ocular vascular meshwork and the retinal tissues and prevents leakage into the retina of macromolecules and other potentially noxious agents as previously reported. The inner BRB (iBRB) is formed by the tight junctions between the capillary endothelial cells and Muller cells. The outer BRB (oBRB) is consisted by tight junctions between cells of RPE and the Bruch's membrane separates the neural retina from the choriocapillaris and is essential for transporting nutrients from the blood to the outer retina. Toxic products from the degenerating retina are suggested as a possible cause of breakdown of the BRB (Spalton DJ et al., 1978; Ivanova E et al., 2019).

Retinal bullae formation has not been reported in humans with the analogous condition, retinitis pigmentosa as far as the authors can tell. However, cystoid macular edema does occur in up to 50% of RP patients further reducing visual function (Strong S et al, 2017). In contrast to the findings in dogs in this study human patients with cystoid macular edema have fluid accumulation within retinal layers rather in the subretinal space (Strong S et al, 2017; Lingao MD et al., 2016).

The fact that not all the PRA- affected dogs in the three groups developed bullae suggests the need for additional factors that could include environmental influences or background genetics. To investigate the latter possibility, we sequenced the BEST1 gene in affected dogs to screen for coding variants. Mutations in BEST1 cause canine multifocal retinopathy which is characterized by multiple retinal focal detachments (Guziewicz KE et al., 2007; Zangerl B et al., 2010). No variants that changed predicted coding were detected. Further studies are required to understand the additional factors that lead to bullae formation and why it occurs in these three forms of PRA. Although not reported in other forms of PRA, it is possible that lesions might develop transiently in the early stages of PRA in other breeds of dog. Once retinal thinning is established the bullae seem to resolve meaning that many dogs diagnosed with PRA in the clinic have more advanced disease than the dogs in this study when they were identified with bullae. The authors have seen dogs of other breeds with multiple bullae that have gone on to develop generalized retinal degeneration (SPJ un published observations). It is also tempting to speculate whether dogs with more advanced PRA that have retinal regions with more advanced retinal degeneration could have previously had bullae in those regions.

2.5 CONCLUSION

In conclusion, veterinarians should be aware that retinal bullae can develop in some forms of PRA and occur prior to retinal thinning and that they are no longer apparent once retinal degeneration is established. The retina in the affected region appears to degenerate more rapidly than in the adjacent regions not affected by bullae. SD- OCT is a sensitive tool for detecting these bullae.

2.6 ACKNOWLEDGMENTS

The authors would like to thank Janice Querubin for excellent animal handling.

2.7 CONFLICT OF INTERESTS

The authors declare no conflicts of interest.

REFERENCES

PETERSEN- JONES SM, KOMAROMY AM. Dog models for blinding inherited retinal dystrophies. **Hum Gene Ther Clin Dev**. 2015; 26:15- 26.

PETERSEN JONES SM, MOWAT FM. Diseases of the canine ocular fundus. In: Gelatt KN, Ben-Shlomo G, Gilger BC, Hendrix DVH, Kern TJ, Plummer CE eds. **Vet Ophthalmol**, (6th ed, 1477–1574). John Wiley & Sons, Inc.; 2021.

ROPSTAD EO, BJERKAS E, NARFSTRÖM K. Clinical findings in early onset cone- rod dystrophy in the Standard Wire- haired Dachshund. **Vet Ophthalmol**. 2007; 10:69- 75.

GOLDSTEIN O, MEZEY JG, BOYKO AR, et al. An ADAM9 mutation in canine cone- rod dystrophy 3 establishes homology with human cone- rod dystrophy 9. **Mol Vis**. 2010; 16:1549- 1569.

WINKLER PA, EKENSTEDT KJ, OCCELLI LM, et al. A large animal model for CNGB1 autosomal recessive retinitis pigmentosa. **PLoS One**. 2013;8: e72229.

SUDHARSAN R, SIMONE KM, ANDERSON NP, AGUIRRE GD, BELTRAN WA. Acute and protracted cell death in light- induced retinal degeneration in the canine model of rhodopsin autosomal dominant retinitis pigmentosa. **Invest Ophthalmol Vis Sci**. 2017; 58:270- 281

SOMMA AT, DUQUE MORENO JC, SATO MT, et al. Characterization of a novel form of progressive retinal atrophy in Whippet dogs: a clinical, electroretinographic, and breeding study. **Vet Ophthalmol**. 2017;20: 450- 459.

DUFOUR VL, CIDECIYAN AV, YE GJ, et al. Toxicity and efficacy evaluation of an adeno- associated virus vector expressing codon- optimized rpgr delivered by subretinal injection in a canine model of X- linked retinitis pigmentosa. **Hum Gene Ther**. 2020; 31:253- 267.

MARINHO LLP, OCCELLI LM, PASMANTER N, SOMMA AT, MONTIANI- FERREIRA F, PETERSEN- JONES SM. Autosomal recessive night blindness with progressive photoreceptor degeneration in a dog model. **Invest Ophthalmol Vis Sci**. 2019;60: 465.

PETERSEN- JONES SM, OCCELLI LM, WINKLER PA, et al. Patients and animal models of CNGbeta1- deficient retinitis pigmen tosa support gene augmentation approach. **J Clin Invest**. 2018;128: 190- 206.

GUZIEWICZ KE, ZANGERL B, LINDAUER SJ, et al. Bestrophin gene mutations cause canine multifocal retinopathy: a novel animal model for best disease. **Invest Ophthalmol Vis Sci**. 2007; 48:1959- 1967.

ZANGERL B, WICKSTROM K, SLAVIK J, et al. Assessment of canine BEST1 variations identifies new mutations and establishes an independent bestrophinopathy model (cmr3). **Mol Vis**. 2010;16: 2791- 2804.

WINKLER PA, RAMSEY HD, PETERSEN- JONES SM. A novel mutation in PDE6B in Spanish Water Dogs with early- onset progressive retinal atrophy. **Vet Ophthalmol**. 2020;23: 792- 796.

MAGNUSSON H. Über retinitis pigmentosa und Konsinguinität beim Hunde. **Arch Vergl Ophthalmol**. 1911;2: 147- 163.

AGUIRRE GD, FARBER D, LOLLEY R, FLETCHER RT, CHADER GJ. Rod- cone dysplasia in Irish setters: a defect in cyclic GMP metabolism in visual cells. **Science**. 1978;201: 1133- 1134.

OSINCHUK SC, LEIS ML, SALPETER EM, SANDMEYER LS, GRAHN BH. Evaluation of retinal morphology of canine sudden ac quired retinal degeneration syndrome using optical coherence tomography and fluorescein angiography. **Vet Ophthalmol**. 2019;22: 398- 406.

OH A, FOSTER ML, WILLIAMS JG, et al. Diagnostic utility of clinical and laboratory test parameters for differentiating between sudden acquired retinal degeneration syndrome and pituitary-dependent hyperadrenocorticism in dogs. **Vet Ophthalmol**. 2019;22: 842- 858.

GROZDANIC SD, LAZIC T, KECOVA H, MOHAN K, KUEHN MH. Optical coherence tomography and molecular analysis of sudden acquired retinal degeneration syndrome (SARDS) eyes suggests the immune- mediated nature of retinal damage. **Vet Ophthalmol**. 2019; 22: 305- 327.

AMER R, NALCI H, YALCINDAG N. Exudative retinal detachment. **Surv Ophthalmol**. 2017;62: 723- 769.

GUZIEWICZ KE, SINHA D, GOMEZ NM, et al. Bestrophinopathy: an RPE- photoreceptor interface disease. **Prog Retin Eye Res**. 2017;58: 70- 88.

SPALTON DJ, RAHI AH, BIRD AC. Immunological studies in retinitis pigmentosa associated with retinal vascular leakage. **Br J Ophthalmol**. 1978;62: 183- 187.

IVANOVA E, ALAM NM, PRUSKY GT, SAGDULLAEV BT. Blood- retina barrier failure and vision loss in neuron- specific degeneration. **JCI Insight**. 2019; 5: e126747.

STRONG S, LIEW G, MICHAELIDES M. Retinitis pigmentosa- associated cystoid macular oedema: pathogenesis and avenues of intervention. **Br J Ophthalmol**. 2017; 101:31- 37.

LINGAO MD, GANESH A, KARTHIKEYAN AS, et al. Macular cystoid spaces in patients with retinal dystrophy. **Ophthalmic Genet**. 2016;37(4):377- 383.

3 EVALUATION OF HEALING, THICKNESS, AND CORNEAL TRANSPARENCY AFTER CROSSLINKING IN DOGS WITH DEEP AND DEGRADED ULCERS

ABSTRACT

Melting Keratitis is an ophthalmic emergency in dogs and can lead to vision loss especially in brachycefalic dog breeds. Therapies aimed at eradicating the progression and preserve the transparency of the tissue. When intensive clinical treatment fails, PACK-CXL is a rational option and has been largely studied in the last two decades due to promising results. CXL is a photodynamic therapy using Riboflavin (VitB2) that destroy microorganisms, increases the biochemical strength, reduce the biodegradation and stabilizes the cornea by forming new crosslinking in the corneal stroma. The objective of this study was to evaluate the healing, compare the corneal thickness using ultrasonic pachymetry (UP) and UBM ultrasound as well as evaluation of the corneal transparency using the UBM images and software ImageJ® after PACK-CXL in infected and degraded ulcers in dogs. The 24 treated eyes were re-epithelized up to 30 days. No statistical difference in thickness was observed between treated and control eyes using UP differently of UBM measurements. When compared thickness in both techniques, delta different from zero was observed in all subgroups. Regarding opacity, the difference was statistically significant between the groups. It is well evident that the eyes of the study are in general more opaque compared to the measures of contralateral eyes (control) even considering only the stroma or stroma plus epithelium. In conclusion, the VET-CXL protocol may represent a cost-effective and adjunctive therapy for infectious ulcers in dogs, Ultrasonic Pachymetry and Ultrasound Biomicroscopy (UBM) are reliable methods of determination of corneal thickness despite the statistical difference between the techniques in the present study, UBM allows for high resolution imaging for opacity using ImageJ software evaluation and quantification. Further randomized and controlled investigation is required to better understand the evidence base in this field.

Keywords: Melting keratitis. Crosslinking. Ultrasonic pachymetry. Ultrasound biomicroscopy.

3.1 INTRODUCTION

A corneal ulcer is an open sore or lesion on the cornea which is the dome-shaped front surface of the eye. They can be classified according to the etiology and depth of corneal involvement and be caused by primary ocular surface disorders, such as SCCED (Spontaneous Chronic Corneal Epithelial Defects), or secondary ocular surface disorders, such as keratitis. Ulcerative Keratitis is one of the major ophthalmic diseases in dogs and is a potentially sight-threatening condition of the cornea often presenting as an ophthalmic emergency requiring prompt medical attention to prevent Keratomalacia, melting keratitis, other complications and vision loss (Marcato PS., 2015; Jones DB., 1981).

Melting keratitis or keratomalacia is a serious condition that occurs with relative frequency in veterinary ophthalmology, especially in predisposed brachycephalic (short-nosed) dog breeds with compromised ocular anatomy. Brachycephalic dogs have an odds ratio of 6 for developing infectious keratitis, compared to typical mesocephalic or dolichocephalic dogs (O'Neill DG et al., 2017; Packer RM et al., 2015; Marlar AB et al., 1994; Massa KL et.al., 1999; Gilger BC, 2007; Kern TJ, 1990). Corneal melting results from the enzymatic degradation of stromal collagen by matrix

metalloproteinases (MMPs), which are released endogenously and exogenously and an imbalance between these proteolytic enzymes and the proteinase inhibitors present in the cornea and the precorneal tear film often caused by a secondary bacterial or fungal corneal infection. It is also referred to as corneal melting, due to its typical gelatinous appearance resulting from stromal collagen degradation.

Besides that, systemic immune-mediated diseases, topical medications, and previous ocular conditions can also lead to melting in the absence of infection, affecting the balance of the scar response through the production of collagenolytic agents by resident and inflammatory cells. Therefore, progression of both keratomalacia and infectious keratitis may result in significant corneal scarring and corneal perforation, ultimately threatening vision and loss of the globe (Ollivier FJ et al., 2003; Ollivier FJ et al.,2007; Fini ME, Girard MT, 1990; Perez VL et al., 2002; Marcon AS et al., 2003; Geerling G et al., 1999).

Treatment of corneal ulcers aims to eradicate the underlying cause and reduce inflammation and the ocular immune response in order to preserve the transparency of the tissue as much as possible. Intensive treatment with topical antimicrobials to treat a potential infection and anti-collagenase therapy is initiated to try to mitigate collagen loss and retain as much corneal tissue as possible to stop progression of the melting process. Topical anti-collagenase treatments in veterinary ophthalmology include EDTA, acetylcysteine, autologous serum, plasma, fresh frozen plasma (FFP), freeze–thaw cycled plasma (FTCP), and platelet-rich plasma (PRP).

To guide specific antimicrobial therapy, culture with susceptibility testing, PCR, and cytological evaluation to undertake reliable therapy and contain the evolution of the antibiotic resistance phenomenon is recommended. The World Health Organization has declared antimicrobial resistance one of the major public health threats of the twenty-first century (Ollivier FJ et al., 2003; Gilger N, 2007; World Health Organization, 2014; Garg Prashant et al., 2017). Due to the pain involved, analgesic treatment with NSAIDs, opioids and paracetamol may be required.

In case of clinical treatment failure or other ocular co-morbidities may require additional treatments such surgeries to prevent corneal scaring and vision loss including Corneal Crosslinking (CXL) (Spiess BM et al., 2013).

Natural covalent cross-links represent a physiological mechanism between the corneal collagen fibers responsible for the improvement of the biomechanical stability of the cornea. Corneal collagen cross-linking was developed in the late 1990s to increase the stability and reduce the biodegradation of the corneal collagen matrix in primary and secondary corneal ectatic diseases, most precisely keratoconus (Spoerl E et al., 2007; Wollensak G et al., 2003). The CXL is a photodynamic therapy which consists in the administration of an ophthalmic solution enriched with riboflavin (vitamin B2) followed by irradiation of the cornea with ultraviolet A light (UV-A) (Maier Philip., et al., 2019; Moghadam., et al., 2019) riboflavin (vitamin B2) acts as photosensitizer when exposed to UV-A light with a wavelength of 370 nm creating new chemical bonds in the stroma matrix via photopolymerization. CXL increases the biochemical strength and stabilizes the cornea

by forming new crosslinks in the corneal stroma between collagen fibers and proteoglycan core proteins resulting in an increased collagen packing density, more resistant to enzymatic digestion, modulation of melting and bacterial colonization through steric hindrance. Additionally, the free radicals induced by CXL directly damage and destroy microorganisms and lead to apoptosis of cells in the irradiation area (Spoerl E et al., 1998; Spoerl E et al., 2004; Wollensak G et al., 2004).

The first CXL protocol used for the treatment of keratoconus, known as Dresden protocol, made use of 3 mW/cm^2 UV-A irradiation for 30 minutes for a total UV-A energy dose of 5.4 J/cm^2 to the corneal tissue. In 2008, the Dresden protocol was first tested effectively in humans with infectious keratitis. Initially, only patients with infectious keratitis refractory to medical therapy were treated. Due to the clear difference in disease progression between keratoconus and infectious keratitis, the use of routine keratoconus-tailored CXL protocols may not be optimal for treating infectious keratitis. In 2013, the name Photoactivated Chromophore for keratitis Corneal Cross-linking (PACK-CXL) was adopted at the 9th CXL Congress in Dublin. The modified technique consists based on the Bunsen-Roscoe law of photochemical reciprocity; the same photochemical effect could be obtained by keeping the total energy dose constant while reducing the irradiation time and increasing the irradiation density. In 2014, the first studies that described the use of PACK-CXL in companion animals were published (Tabibian D et al., 2015; Pot SA et al., 2014, Famose F, 2014). Additionally, antimicrobial activity of PACK-CXL against various bacterial, fungal and parasitic (amoeba) agents has been demonstrated *in vitro* and *in vivo* and tested to define the best PACK-CXL settings against various pathogens and at different infection keratitis stages. The use of CXL as an adjunctive therapy for the treatment of melting keratitis may become its major indication in veterinary medicine and the consisted phototherapy protocol of 30mW/cm^2 UV-A power irradiance for 3 minutes with a total emitted energy dose of 5.4 J/cm^2 was validated in the laboratory for exclusive use in veterinary medicine (VET-CXL® protocol) (Razmjoo et al., 2017; Famose, 2016; Huang Jinrong et al., 2018)

Multiple modalities exist to measure corneal thickness during the pre and postoperative evaluation to CXL therapy. Ultrasonic pachymetry typically measures a single point, usually performed in the center of the cornea in many species including dogs, which is considered widely used, accurate, reliable, and the gold standard technique. Ultrasonic pachymetry determines corneal thickness based on the time difference between ultrasound waves reflecting from the anterior and posterior surfaces of the cornea, and accurate results are dependent upon the pachymeter being set to the appropriate velocity of sound for the measured tissue (Demirbas NH, Pflugfelder SC, 1998; Sherwin T, Brookes NH, 2004; Alario AF, Pirie CG, 2014)

Other methods include ultrasound biomicroscopy (UBM), which becomes more widely available and also used to assess many ocular parameters and disorders of the anterior segment because has proven to be a valuable diagnostic tool for evaluation of corneal and scleral disorders, anterior segment masses, the iridocorneal angle and ciliary cleft, as well as lens disorders in both human and animal patients. Based on the ease of portability and increasing affordability, UBM has

become a practical advanced imaging technique for use in animals. Others corneal imaging methods include optical coherence tomography (OCT), and corneal topography systems like Orbscan II and Pentacam which can also provide corneal thickness maps, offering additional information about corneal shape and thickness variations.

Corneal opacity in dogs can be subjective measured and classified based on the extent and characteristics of the clouding. A common method involves a grading scale, often from 0 to 3 or 4, where 0 represents a clear cornea and higher numbers indicate increasing levels of opacity (Bentley E et al., 2003; Gibson TE et al. 1998). Other methods involve assessing the impact on vision and using specialized imaging techniques such ultrasound biomicroscopy (UBM). UBM is a valuable tool for measuring corneal opacity, particularly in cases where the cornea is opaque or when detailed visualization of the anterior segment is needed. UBM uses high-frequency ultrasound waves (50-100 MHz) to create detailed images of the cornea and surrounding structures, allowing for accurate measurement of corneal thickness, the depth and quantification of opacities. This is especially useful in congenital corneal opacities (CCO) and other anterior segment pathologies where direct visualization may be limited (Bentley E et al., 2003; Gibson TE et al. 1998).

The objective of this study was to evaluate the healing, compare the corneal thickness using ultrasonic pachymetry and UBM ultrasound as well as evaluation of the corneal transparency using the UBM images and software ImageJ® after PACK-CXL in infected and degraded ulcers in dogs.

3.2 MATERIALS AND METHODS

3.2.1 Animals

Forty-eight eyes from 24 dogs with unilateral progressive corneal ulcer were prospectively enrolled in this interventional study between August 2022 and June 2025. The average of age was 6.8 years with a range of 2 to 13 years. Twelve of the 24 participants were females (50%) while 12 (50%) were males being 17 (70%) brachycephalic breed dogs. All treatments were performed at the Pompeo Oftalmologia Veterinaria clinic, located in Santos, state of São Paulo-Brazil, after obtaining the owner's consent. All procedures were in accordance with the ARVO Declaration for the Use of Animals in Ophthalmic and Vision Research and were in accordance with the animal protocols institutionally approved by the Department of Ophthalmology of Veterinary Medicine, Federal University of Paraná, Curitiba, Paraná, Brazil.

3.2.2 Pre-treatment examination

The pre-treatment analysis included slit-lamp examination, fluorescein staining, and photography. Culture and sensitivity samples were not collected from all dogs due to previously initiated antibiotic therapy and economic aspects. The diagnosis of corneal melting was based on

a subjective assessment of stromal stability/melting activity, ulcer depth, the aspect of changes in corneal contours and the appearance of degradation in the ulcerated area including the presence of cellular infiltrates.

3.2.3 Crosslinking (CXL)

Under inhalational anesthesia with isoflurane and the application of a topical anesthetic (Proximetacaine 0,5% or oxybuprocaine 0.4%) to the affected corneas, using a surgical microscope (DFVasconcelos MU-M19) the corneal epithelium was removed carefully with cotton swabs and cellulose sponge as much as necessary, depending on the size of the infiltrate and ulcer. A cellulose sponge was also used for subjective tactile evaluation of stromal stability. After insertion of an eyelid speculum, 10 drops of pre-loaded glass syringe Peschke® M Standard 0.1% isoosmolar riboflavin without Dextran were administered every 2 minutes for 20 minutes. Successful penetration of riboflavin into the anterior chamber was confirmed with a slit lamp. The cornea was illuminated using a UV-A lamp PXL VELVET 345 (Peschke Meditrade GmbH, Switzerland), 365-nm ultraviolet A with an irradiance of 30 mW/cm^2 for 3 minutes and a total dose of 5.4 J/cm^2. The diameter of the irradiation was between 9 and 11 mm, depending on the size of the infiltrate, and special care was taken not to irradiate the corneal limbus, as this area contains corneal epithelial stem cells, which are crucial for the re-epithelialization of the corneal surface. During the 5-min irradiation period, the cornea was moistened every minute with isoosmolar 0.1% riboflavin solution. The UV light fell on the corneal surface at a distance of 5 cm in all patients using a caliper to measure. Afterwards, the operated eyes were closed with third eyelid flap. All surgical room professionals were wearing UV-A protection googles during the treatment and the contralateral eyes of the patient were shielded to avoid visual complication.

3.2.4 Post-treatment examination and follow-up

Medical therapy with topical antibiotics (up to 8 times per day), anticollagenases drops (4 times per day), 0,15% Sodium Hyaluronate (4 times per day), blood serum (4 times per day), 5% NACL hyperosmotic (up to 4 times per day as needed) was continued until complete corneal healing. Additionally, oral non-steroidal anti-inflammatory drugs (for 5 days), antibiotics (up to 10 days), analgesics (as needed, for up to 5 days), and fish oil (for 30 days) were administered in all patients after CXL treatment because discontinuation of medical treatment was considered unethical in light of the little-known efficacy of isolate CXL treatment in dogs with severe and infected corneal ulcers. Afterwards the complete healing, medical therapy with topical Ciclosporin 0,5% or Tacrolimus 0,03% drop once a day and Prednisolone acetate 1% twice a day were prescribed per 10 days to minimize the sequelae of dry eye and improve the scar appearance. Post-treatment examinations were performed on day 1 and days 4, 7, 14, 21 and 30 after surgery and at various time points during long-term follow-up. The suture of the third eyelid flap was removed between day 21st and 30th and complete healing was defined as re-epithelialization of

the corneal epithelial defect with disappearance of hypopyon with no anterior chamber activity and clearing of stromal infiltrate. All complications, including perforation of the corneal stroma, were recorded. The available follow-up ranged from 2 to 24 months and included slit-lamp examination, fluorescein staining, and photographic documentation during all reexaminations.

3.2.5 Ultrasonic pachymeter

After the application of topical anesthetic (Proximetacaine 0,5% or oxybuprocaine 0.4%), a lightweight handheld ultrasonic pachymeters (ReichertR iPacR) with 10,5 MHz of frequency was used to measure the corneal thickness of the center of the lesion on the treated area and the similar position in the contralateral eye. iPacR features an advanced filtering algorithm that ensures accurate central corneal thickness (CCT) measurements over a wide range of corneal thicknesses measurements. It takes 25 corneal measurements in rapid succession at a single location and calculates the average thickness and standard deviation. The procedure was repeated three times in each eye and the values and averages were recorded for being used in the statistical analysis.

3.2.6 Ultrasound biomicroscopy

After the application of topical anesthetic (Proximetacaine 0,5% or oxybuprocaine 0.4%), a commercially available ultrasound biomicroscope (Accutome UBM plus, Keeler, USA) with a 48-MHz linear transducer probe connected directly to a laptop computer was used and filled with sterile water was used to acquire images of both eyes of each included dog. Vidisic® Eye Lube (Bausch&Lomb, Brazil) was used as a coating agent. Transcorneal ultrasonography was performed with the probe positioned perpendicular to the globe such that the corneal epithelium, Descemet's membrane-corneal endothelial complex, and anterior lens capsule were of similar echogenicity, confirming perpendicular placement at the time of image acquisition.

Images of the operated area horizontally and vertically from both eyes were obtained in triplicate. The technique was used to measure the thickness using the manufacture software tools and compared to the pachymeter ultrasound values. Besides that, evaluate the corneal opacity using the ImageJ software to evaluated the UBM images acquired.

3.2.7 Ultrasound Pachymeter and Ultrasound Biomicroscopy statistical analysis

Ultrasound Pachymeter and Ultrasound biomicroscopy exams were performed on different visits to optimize the accuracy of each method as well as minimize excess of animal stress and the risk of accidental aspects. Average and corneal thickness measurements were recorded with standard deviation. Statistically significant differences in corneal thickness from ultrasonic pachymeter and Ultrasound UBM measurements were evaluated with a paired student's t test. By convention, statistical significance was determined by a P value. Bland-Altman analyses were performed to assess agreement between modalities. To assess for repeatability of measurements within a modality between study timepoints, Pearson correlation coefficients were calculated.

3.2.8 Data Analysis

To obtain UBM metrics the images were analyzed using the ImageJ software. With it, thickness metrics were computed using the straigh line tool after calibrating the image resolution. Three measurements were made on each image and averaged. Additionally, opacity values were obtained from the images by defining a rectangular region in the zone of interest and calculating the average pixel intensity inside the rectangle. Two sets of measurements were made, one fitting the largest possible rectangle inside the stroma; and one fitting the largest possible rectangle including the stroma and epithelium. In each case, the intensity is expressed as arbitrary units as it represents the gray-scale level of the image given the specific set of hardware acquisition parameters (such as gain). Those parameters were kept fixed for all animals.

Continuous variables were expressed as means ± standard deviations (SD). Initially, for each animal, the difference (delta) between the thickness of the study eye and the fellow obtained by pachymetry was calculated. Deltas are always computed as the study eye minus the fellow eye. The hypothesis that these deltas have a median different from zero (i.e., they have different thickness) was tested using the Sign Test, while the difference between the measurement means was analyzed with the paired t-test. When applicable, the relationship between study and control eye thicknesses was assessed using Pearson's correlation coefficient (linear association) and Spearman's rank correlation coefficient (monotonic association).

Additionally, the mean values obtained by pachymetry were compared with two distinct measurements obtained by ultrasound biomicroscopy. These comparisons were performed for the entire dataset as well as separately for study eyes and control eyes. Again, delta values were calculated, the paired t-test was applied to evaluate differences in means, the Sign Test to assess differences in the delta medians, and Pearson's and Spearman's correlation coefficients were calculated. Agreement between techniques was analyzed using the Intraclass Correlation Coefficient (ICC), specifically ICC (2,1) (two-way random effects, absolute agreement). Furthermore, Bland–Altman plots were constructed, displaying the mean difference, limits of agreement (±1.96 SD) and their respective confidence intervals, as well as scatter plots with identity lines to visually illustrate the proximity between methods.

All analyses were performed using the Python programming language, with statistical and data visualization libraries (pandas, scipy, matplotlib, seaborn). Values of $p < 0.05$ were considered statistically significant.

3.3 RESULTS

3.3.1 Clinical aspects

Crosslinking (CXL) technique was applied in 24 dogs with unilateral severe corneal melting of unknown cause, as described in the Materials and Methods section. Based on a subjective assessment of stromal stability/melting activity, ulcer depth, the aspect of changes in corneal contours and the appearance of degradation in the affected area including the presence of cellular infiltrates, all operated eyes showed for being healed with negative fluorescein test and the stroma stable at the moment of the third eyelid removal around 21st day after the surgery. Presence of corneal opacity, vascularization and pigmentation differ between the patients as well as the pre and post medications. The summary of the pre and postoperative characteristics of the animals, medical treatment and healing aspects are described in the table 1.

	Breed	Eye	Age	Gender	Post-CXL Treatment	Flap removal	Negative fluorescein	Glaucoma	Perfuration
Dog 1	Shihtzu	OS	13y6m	female	Gatifloxacin Q2-6H K-EDTA 0,35% QID 0,15% Sodium Hyaluronate 5% NACL drop QID per 10 days Prednisolone acetate 1% drop Tacrolimus 0.03% SID Meloxican* Amoxiciln Fish oil	23 days	23 days	no	no
Dog 2	Shihtzu	OS	7y	female	Moxifloxacin Q2-6H K-EDTA 0,35% QID 0,15% Sodium Hyaluronate Prednisolone acetate 1% drop Tacrolimus 0.03% SID Meloxican* Amoxiciln Fish oil + Lutein	24 days	24 days	no	no
Dog 3	Shihtzu	OS	2y1m	male	Gatifloxacin Q2-6H K-EDTA 0,35% QID 0,15% Sodium Hyaluronate 5% NACL drop QID per 10 days Prednisolone acetate 1% drop	20 days	20 days	no	no

					Meloxican* Amoxiciln Fish oil				
Dog 4	SRD	OD	10y	female	Gatifloxacin Q2-6H K-EDTA 0,35% QID 0,15% Sodium Hyaluronate Serum QID Prednisolone acetate 0,1% drop Carprofen Amoxiciln Fish oil	20 days	20 days	no	no
Dog 5	Shihtzu	OD	3y	male	Moxifloxacin Q2-6H K-EDTA 0,35% QID 0,15% Sodium Hyaluronate Prednisolone acetate 1% drop Ciclosporina 0,5% drop Meloxican* Amoxiciln Dipirone	19 days	19 days	no	no
Dog 6	Shihtzu	OS	3y3m	male	Gatifloxacin Q2-6H K-EDTA 0,35% QID 0,15% Sodium Hyaluronate Diclofenac sodium 0.1% Ciclosporina 0,5% drop Meloxican* Enrofloxacin	31 days	31 days	no	no
Dog 7	SRD	OD	12y	female	Gatifloxacin Q2-6H K-EDTA 0,35% QID 0,5% Sodium Carmelose Prednisolone acetate 1% drop Carpofen* Doxyciclin Fish oil	35 days	35 days	yes	yes
Dog 8	Shihtzu	OD	2y8m	female	Gatifloxacin Q2-6H K-EDTA 0,35% QID 0,5% Sodium Hyaluronate Meloxican* Amoxicilin Fish oil	21 days	21 days	no	no
Dog 9	Pinscher	OD	14y5m	female	Gatifloxacin Q2-6H K-EDTA 0,35% QID 0,5% Sodium Carmelose	24 days	24 days	no	no

					Serun Carprofen* Amoxicilin Dipirone Fish oil				
Dog 10	Pug	OS	5y4m	female	Moxifloxacin Q2-6H K-EDTA 0,35% QID 0,15% Sodium Hyaluronate Diclofenac sodium 0.1% drop Tacrolimus 0.03% Meloxican* Amoxiciln Dipirone Fish oil	26 days	26 days	no	no
Dog 11	Standforbull terrier	OS	2y	male	Gatifloxacin Q2-6H K-EDTA 0,35% QID 0,15% Sodium Hyaluronate 0,4% Trometamol Cetorolac drop Ciclosporina 0,5% drop Prednisolone acetate 1% drop Meloxican* Amoxicilin Dipirone Fish oil	27 days	27 days	no	no
Dog 12	Shihtzu	OD	11y10m	female	Moxifloxacin Q2-6H K-EDTA 0,35% QID 0,15% Sodium Hyaluronate Prednisolone acetate 1% drop Ciclosporina 0,5% drop 2,5% Cefazolin drop Carprofen* Amoxiciln Dipirone Fish oil	27 days	27 days	no	yes
Dog 13	Shihtzu	OS	5a11m	male	Gatifloxacin Q2-6H K-EDTA 0,35% QID 0,15% Sodium Hyaluronate Prednisolone acetate 1% drop Carpofen* Enrofloxacin Fish oil	15 days	15 days	no	no
Dog 14	Shihtzu	OS	4y	male	Gatifloxacin Q2-6H K-EDTA 0,35% QID	24 days	24 days	no	no

					0,15% Sodium Hyaluronate Prednisolone acetate 1% drop Ciclosporina 0,5% drop Carpofen* Doxyciclin Tramadol Fish oil				
Dog 15	Boxer	OS	9y2m	male	Ofloxacin Q2-6H K-EDTA 0,35% QID 0,5% Sodium Carmelose 5% NACL drop QID per 10 days Prednisolone acetate 1% drop Diclofenac Sodium 0.1% drop Ciclosporina 0,5% drop Carpofen* Doxyciclin Fish oil	23days	23days	no	no
Dog 16	Shihtzu	OS	11m	female	Moxifloxacin Q2-6H K-EDTA 0,35% QID 0,15% Sodium Hyaluronate Prednisolone acetate 1% drop Ciclosporina 0,5% drop Meloxican* Amoxiciln Dipirone	24 days	24 days	no	no
Dog 17	Shihtzu	OS	4y1m	female	Gatifloxacin Q2-6H K-EDTA 0,35% QID 0,15% Sodium Hyaluronate Serum QID Prednisolone acetate 0,1% drop Carprofen Amoxiciln Fish oil	20 days	20 days	no	no
Dog 18	Shihtzu	OS	9y 5m	male	Gatifloxacin Q2-6H K-EDTA 0,35% QID 0,15% Sodium Hyaluronate 5% NACL drop QID per 10 days Prednisolone acetate 1% drop Meloxican* Amoxiciln Fish oil	23 days	23 days	no	no
Dog 19	Buldogue	OS	10y	male	Moxifloxacin Q2-6H K-EDTA 0,35% QID	31 days	31 days	no	no

					0,15% Sodium Hyaluronate Prednisolone acetate 1% drop Tacrolimus 0.03% SID Meloxican* Amoxiciln Fish oil + Lutein				
Dog 20	Shihtzu	OS	2y4m	male	Gatifloxacin Q2-6H K-EDTA 0,35% QID 0,15% Sodium Hyaluronate 5% NACL drop QID per 10 days Prednisolone acetate 1% drop Tacrolimus 0.03% SID Meloxican* Amoxiciln Fish oil	35 days	35 days	no	no
Dog 21	Shihtzu	OS	5y1m	male	Gatifloxacin Q2-6H K-EDTA 0,35% QID 0,5% Sodium Hyaluronate Meloxican* Amoxicilin Fish oil	20 days	20 days	no	no
Dog 22	Pinscher	OD	12y	female	Gatifloxacin Q2-6H K-EDTA 0,35% QID 0,5% Sodium Carmelose Serun Carprofen* Amoxicilin Dipirone Fish oil	19 days	19 days	no	yes
Dog 23	Shihtzu	OE	10y8m	male	Gatifloxacin Q2-6H K-EDTA 0,35% QID 0,15% Sodium Hyaluronate Diclofenac sodium 0.1% Ciclosporina 0,5% drop Meloxican* Enrofloxacin	21 days	21 days	no	no
Dog 24	Shihtzu	OD	10m	female	Gatifloxacin Q2-6H K-EDTA 0,35% QID 0,5% Sodium Carmelose Prednisolone acetate 1% drop Carprofen* Doxyciclin Fish oil	24 days	24 days	no	no

*Meloxicam was prescribed once daily at 0.1mg/kg and *Carprofen once daily at 4mg/ Kg.

†Doxycycline was prescribed at 10mg/kg once daily† Amoxicilin 15mg/kg twice daily† Enrofloxacin 5mg/kg twice daily

3.3.2 Thickness by Ultrasonic Pachymeter

The mean corneal thickness in the study group was 0.602 ± 98.93 mm (central of the treated area) and 0.582 ± 87.62 mm in the similar location in control group. Despite the mean difference of 0.20 mm, the p value was 0.3885 and no statistical difference was observed between the groups using ultrasonic pachymeter.

When the medial delta thicknesses values between the techniques ultrasound pachymeter and ultrasound biomicroscopy were compared we found the following subgroups results:

General: All eyes (studied + control) of both groups (Pachymeter vs UBM) without distinguishing were compared to make sure techniques agree in either eye. The delta was significantly different from zero (p=0.0002).

Study eye groups (Pachymeter vs UBM): The delta was significantly different from zero (p= 0.0156).

Control eye groups (Pachymeter vs UBM): The delta was significantly different from zero (p=0,0312).

3.3.3 Thickness by Ultrasound Biomicroscopy

The mean ± standard deviation corneal thickness measured by Accutome UBM software was 0.640 ± 0.22 mm (central of the treated area) and 0.518 ± 0.90 mm (similar location in the control eyes). The difference was statistically significant (p=0.018). It is possible to see in the Scatter plot bellow (Figure A) that the measurements of contralateral eyes (controls) are more stables with a tendency for having lower values than the study eye. We also calculated in millimeters the Delta of the thickness (study eye minus control eye thicknesses). Therefore, positive values indicate thicker measures for study eyes. An average of 0.125 ± 0.18 mm was observed and demonstrated in the Scatter plot bellow (Figure B). no statistical difference was observed (p=0,070).

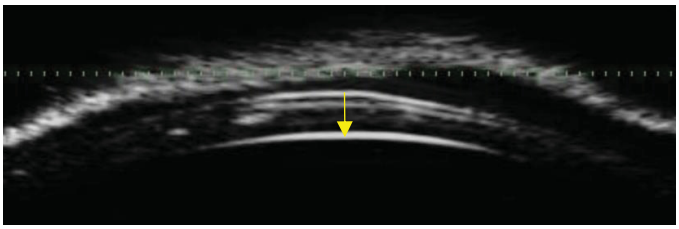

Image 1 - Yellow narrow indicates the axis position for thickness measurement using UBM ultrasound in study control eyes

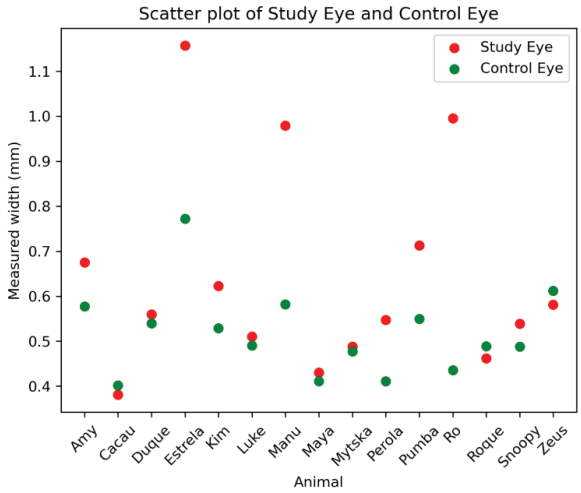

Figure A - Scatter plot showing the thickness difference between Study and Control Eye using UBM ultrasound

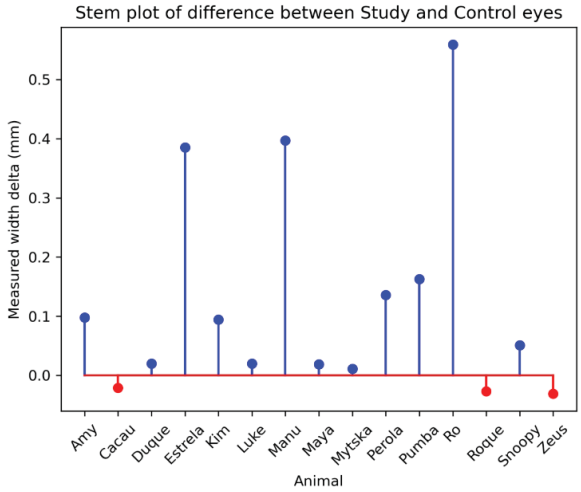

Figure B - Scatter plot showing the Delta of the thickness measurement between study and control eyes.

3.3.4 Corneal Opacity Analysis

The mean ± standard deviation corneal opacity calculated in arbitrary units in the stroma area measured by ImageJ® using UBM image was 47.12 ± 33.69 a.u. (central of the treated area) and 11.78 ± 8.68 a.u. (similar location in the control eyes) respectively. The difference was statistically significant (p=0.003). It is well evident in the scatter plot bellow (Figure C) that the eyes of the study are in general more opaque (14/15 cases, 93.33%) compared to the measures of contralateral eyes (control).

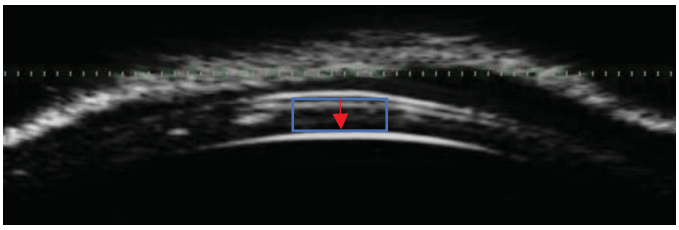

Image 2 - The rectangle in blue indicates the chosen area to measure the stroma opacity in arbitrary units

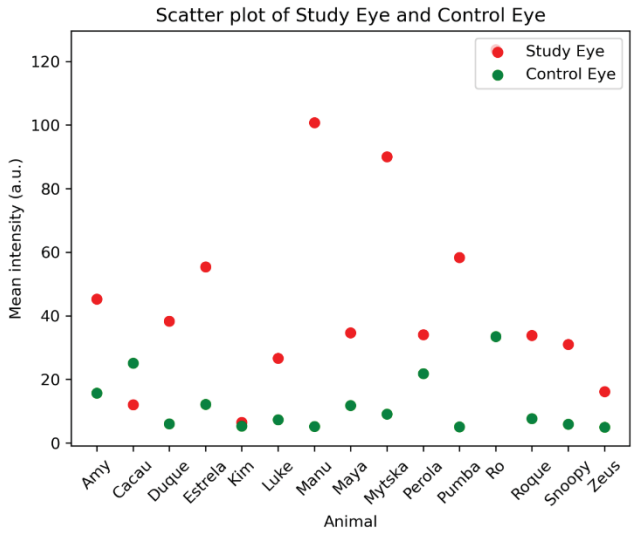

Figure C - Scatter plot showing that the eyes of the study are in general more opaque (14/15 cases, 93.33%) compared to the measures of contralateral eyes (control).

The mean ± standard deviation corneal opacity calculated in arbitrary units in the epithelium plus stroma area measured by ImageJ® using UBM image was 60.99 ± 30.52 a.u. (central of the treated area) and 34.52 ± 13.79 a.u. (similar location in the control eyes). The difference was statistically significant (p=0.012). It is possible to see in the Scatter plot that the measurements of contralateral eyes (control) are more stables with a tendency of having lower values compared to the study eye. The inclusion of the superficial area (epithelium) naturally diluted the difference between the groups. Besides that, the study group still has a tendency of higher values (more opacity) compared to the control group (12/15 cases, 80%).

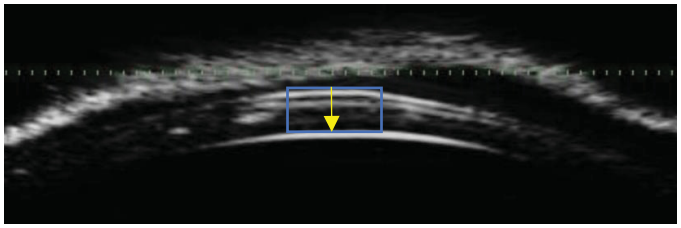

Image 3 - The rectangle in blue indicates the chosen area to measure the epithelium plus stroma opacity in arbitrary units.

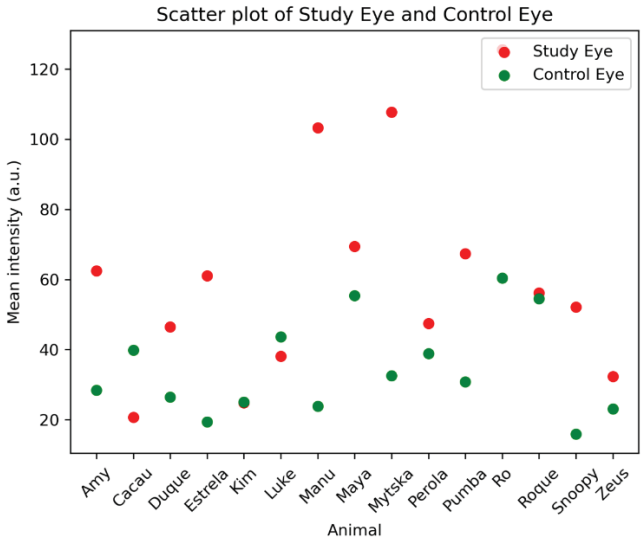

Figure D - Scatter plot showing that the eyes of the study are in general more opaque (12/15 cases, 80%) compared to the measures of contralateral eyes (control).

Delta of both groups considering the opacity was measured (study eye minus control eye opacities) to verify if the median is significant different of zero value. Therefore, positive values indicate more opaque measures. An average of 26.48 ± 29.79 a.u (epithelium plus stroma) and 35.34 ± 32.04 a.u. (stroma) was observed and demonstrated in the Scatter plots bellow. The difference was statistically significant (p=0.004) for the stroma group and not statistically significant for epithelium plus stroma group (p=0.070) possibly because the opacity intensity lost the significance due to the dilution of epithelium inclusion in both groups.

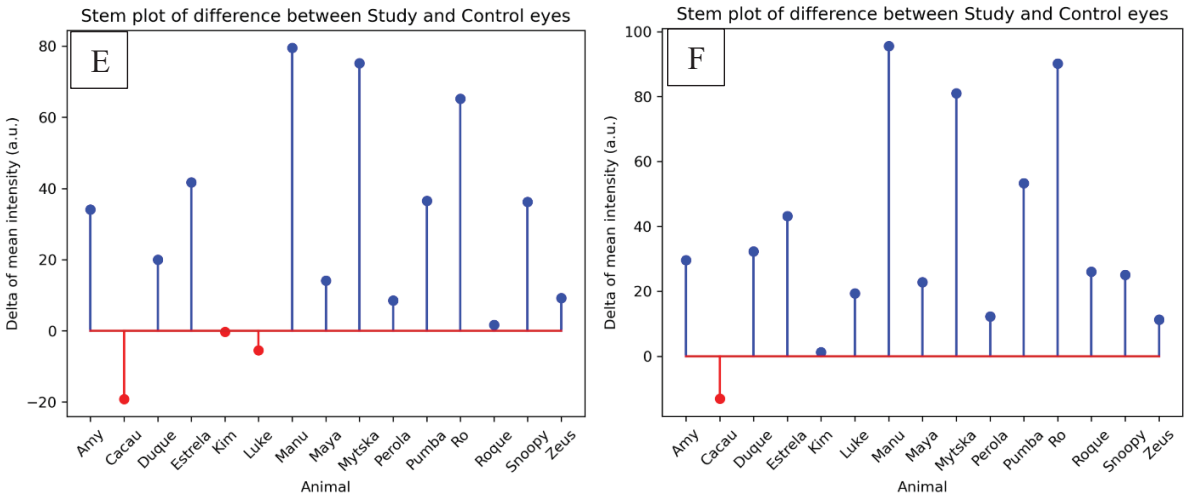

Figure E and F - (E) Scatter plot showing positive values in the epithelium plus stroma group and (F) in the stroma group.

3.4 DISCUSSION

CXL is a technique developed for the treatment of progressive keratoconus in humans (Wollensak G et al., 2003; Raiskup-Wolf F et al., 2008). Posteriorly, extended to bullous keratopathy, LASIK ectasia (Hafezi F et al., 2007), Fuchs' dystrophy (Hafezi F et al., 2010) and, has been largely studied for infectious corneal melting (Iseli et al., 2008; Makdoumi K et al., 2010; Schrier A et al., 2009; Martins AS et al., 2008) due to UV-A light mediated photoactivation of B vitamin results in DNA and RNA damage in viruses, bacteria, fungi, and protozoa (Ito K et al., 1993; Tsugita et al., 1965). CXL increases the corneal rigidity and resistance to collagenases avoiding corneal degradation and progression of infectious melting (Spoerl E et al., 2004, Iseli et al., 2008; Makdoumi K et al., 2010; Anwar HM et al., 2011).

Considering previous researches (Tabibian D et al., 2015; Hafezi F et al., 2023; Knyazer B et al., 2020), this study also demonstrated that the PACK -CXL (Photoactivated Chromophore for Keratitis – Corneal Cross-Linking protocol (30 mW/cm² for 3 minutes)) which is the clinical use of CXL for infectious keratitis associated with medical therapy was effective in promoting healing of infectious and melting corneal ulcers in dogs, suggesting that PACK-CXL can be very useful and are most safe to be used as treatment for infectious keratitis. All studied eyes showed complete re-epithelialization and stromal stabilization by the 21st postoperative day corroborating with the literature (Spiess BM et al., 2014; Famose F et al., 2014). These findings are in agreement with previous studies that highlight the potential of PACK-CXL as an adjuvant therapy for cases refractory to conventional clinical treatment, especially in breeds with anatomical predisposition to corneal collapse, such as brachycephalic dogs (O'Neill DG et al., 2017; Packer RM et al., 2015; Massa KL et.al., 1999; Pot SA et al., 2014).

Measurement of corneal thickness is essential in diagnosing and monitoring animals with corneal diseases or glaucoma being the ultrasound pachymeter the gold standard technique for measurements in humans and veterinary ophthalmology due to the ease of use, reproducibility of measurements and relative cost/availability of handheld ultrasound pachymeters (Alario and Pirie, 2014). Besides that, accurate assessment of corneal thickness prior and after to corneal cross-linking is important since the treatment of corneas with inadequate thickness can lead to endothelial and structural damage (Wollensak G et al., 2003; Spoerl E et al., 2007; Galvis V et al., 2017). Limitations of ultrasonic pachymetry are the direct corneal contact required for measurement, non-perpendicular placement can lead to overestimation of corneal thickness and corneal indentation with the probe could disrupt the reflective surfaces, including displacement of the tear film and cause thinning of the epithelium leading to inaccurate results or different values when compared with other corneal thickness measurements techniques (Spoerl E et al., 2007).

The absence of a statistically significant difference in corneal thickness between studied and control eyes in our study when assessed by ultrasonic pachymetry may suggest that the treatment preserves overall corneal architecture. However, measurements obtained by UBM were significantly different between groups, possibly reflecting greater sensitivity of this method in

detecting subtle morphological changes or residual stromal edema. Similar findings were reported in previous studies in normal dogs but not in infectious melting treated with PACK CXL like ours suggesting that UBM consistently resulted in greater corneal thickness measurements relative to ultrasonic pachymeter which the accuracy in determination of corneal thickness is dependent upon the set velocity of the speed of sound through the measured tissue (Tang J et al., 2011). This discrepancy between techniques has been previously reported and reinforces the importance of using multiple methods for corneal thickness assessment (Martín-Suárez E et al., 2017; Jeong S et al., 2018).

The UBM provides high-resolution images of the tissue of interest such as cornea, sclera, conjunctiva, iris, uvea. Limitations include preferentially sedation of the dog and global contact for quality image acquisition. The increased stromal opacity observed in studied eyes, even after complete healing, was expected given the initial severity of the corneal damage. Residual opacity is a common outcome of the inflammatory response and collagen remodeling following injury, particularly in cases with stromal necrosis. It is a potential complication following corneal crosslinking (CXL) in dogs, though it is often temporary and resolves over time depending the characteristic and depth of the ulcer. This opacity, also known as corneal haze, can result from various factors related to the healing process. While CXL is generally considered a safe and effective treatment for corneal ulcers and other conditions, understanding the physio pathogenesis for opacity and its management is important. Our present study focused on corneal opacity measurements in the post-operative assessment for PACK – CXL.

Quantification of the opacity using UBM combined with image editing software (ImageJ®) proved useful and reproducible, allowing for objective evaluation of a traditionally subjective parameter for both groups revealing a significant difference between the studied and control group. The use of ImageJ was previously described in researches evaluating the action of Losartan in modulation of the therapeutic treatment of established corneal scaring (Villabona-Martinez V et al., 2024) and the effect of vitamin C supplementation on reducing the size of corneal opacity resulting from infectious keratitis (Cho YW et al., 2014) but to our knowledge, no other research evaluating corneal opacity after Pack CXL in corneas with severe corneal degradation in dogs had been performed.

Although the study did not include a control group without CXL treatment for ethical reasons, the results suggest that the PACK-CXL protocol significantly contributed to infection control and stabilization of stromal degradation, in line with previous studies (Famose F et al., 2014; Pot SA et al., 2014).

Standard medical treatment (antibiotics, anticollagenases, lubricants) was maintained in all cases, reflecting real-world clinical practice. This reinforces the role of CXL as an adjunctive, not a replacement, therapy, as recommended in the literature (Spiess BM et al., 2014).

Limitations of this study include the relatively small number of patients, the etiological heterogeneity of the ulcers, and the lack of systematic microbiological cultures in all cases.

Furthermore, long-term follow-up is needed to assess the functional impact of the treatment on visual acuity, which remains a challenge in veterinary ophthalmology.

3.5 CONCLUSIONS

The results described in this study suggest that the VET-CXL protocol may represent a cost-effective and adjunctive therapy for infectious ulcers in dogs, Ultrasonic pachymetry and Ultrasound Biomicroscopy (UBM) are reliable methods of determination of corneal thickness despite the statistical difference between the techniques in the present study, UBM allows for high resolution imaging for opacity using ImageJ software evaluation and quantification and future studies that are randomized and controlled would be necessary to better understand the evidence base in this field.

3.6 ACKNOWLEDGEMENT

Fabiano Montiani-Ferreira, Federal University of Paraná, Curitiba, State of Paraná, Brazil for the intellectual support.

Pompeo Vet. Ophthalmology, Santos, State of São Paulo, Brazil for the casuistry and financial support.

Lucas R. De Pretto for the statistical analysis support.

Thiago Peixoto for the Ultrasound Biomicroscopy (UBM) image acquiring support.

Jorge Pereira for the Ultrasound Pachymeter equipment support.

REFERENCES

MARCATO PS. “Systematic veterinary pathology”. Vol. II, Milano: **Edagricole** (Second edition (2015).

JONES DB. Decision-making in the management of microbial keratitis. **Ophthalmology.** 1981; 88:814–20.

O’NEILL DG, LEE MM, BRODBELT DC, CHURCH DB, SANCHEZ RF. Corneal ulcerative disease in dogs under primary veterinary care in England: epidemiology and clinical management. **Canine Genet Epidemiol**. 2017; 4:5.

PACKER RM, HENDRICKS A, BURN CC. Impact of facial conformation on canine health: corneal ulceration. **PLoS One**. 2015;10(5): e0123827.

MARLAR AB, MILLER PE, CANTON DD et al. Canine keratomycosis: a report of eight cases and literature review. **Journal of the American Animal Hospital Association** 1994; 30: 331–340.

MASSA KL, MURPHY CJ, HARTMANN FA et al. Usefulness of aerobic microbial culture and cytologic evaluation of corneal specimens in the diagnosis of infectious ulcerative keratitis in animals. **Journal of the American Veterinary Medical Association** 1999; 215: 1671–1674.

GILGER BC. Diseases and surgery of the canine cornea and sclera. In: Vet Ophthalmol, 4th edn. (ed Gelatt KN) Blackwell Pub, Ames, Iowa, 2007; 690–752.

KERN TJ. Ulcerative keratitis. **Veterinary Clinics of North America** 1990; 20: 643–666.

OLLIVIER FJ, BROOKS DE, KALLBERG ME et al. Evaluation of various compounds to inhibit activity of matrix metalloproteinases in the tear film of horses with ulcerative keratitis. **American Journal of Veterinary Research** 2003; 64: 1081–1087. Epub 2003/09/19.

OLLIVIER FJ, GILGER BC, BARRIE KP et al. Proteinases of the cornea and preocular tear film. **Veterinary Ophthalmology** 2007; 10: 199 206. Epub 2007/06/15.

FINI ME, GIRARD MT. Expression of collagenolytic/gelatinolytic metalloproteinases by normal cornea. **Investigative Ophthalmology & Visual Science** 1990; 31: 1779–1788. Epub 1990/09/01.

PEREZ VL, AZAR DT, FOSTER CS. Sterile corneal melting and necrotizing scleritis after cataract surgery in patients with rheumatoid arthritis and collagen vascular disease. **Seminars in Ophthalmology** 2002; 4: 124–130. Epub 2003/05/22.

MARCON AS, RAPUANO CJ, TABAS JG. Tissue adhesive to treat 2-site corneal melting associated with topical ketorolac use. **Journal of Cataract and Refractive Surgery** 2003; 29:393–394.Epub2003/03/22.

GEERLING G, JOUSSEN AM, DANIELS JT et al. Matrix metalloproteinases in sterile corneal melts. **Annals of the New York Academy of Sciences** 1999; 878: 571–574. Epub 1999/07/23.

GILGER N. Diseases and surgery of the canine cornea and sclera. In: **Veterinary Ophthalmology**. (ed. Gelatt KN) Blackwell Pub, Ames, Iowa, 2007; 643.

WORLD HEALTH ORGANIZATION. Antimicrobial resistance: global report on surveillance. Geneva: **World Health Organization**. 2014.

GARG PRASHANT et al. “Collagen Cross-Linking for Microbial Keratitis”. **Middle East African Journal of Ophthalmology** 1 (a2017): 18-23.

SPIESS BM, POT SA, FLORIN M et al. Corneal collagen cross-linking (CXL) for the treatment of melting keratitis in cats and dogs: a pilot study. **Veterinary Ophthalmology** 2013; doi: 10. 1111/vop.12027.

SPOERL E, MROCHEN M, SLINEY D et al. Safety of UVA-riboflavin cross-linking of the cornea. **Cornea** 2007; 26: 385–389.

WOLLENSAK G, SPOERL E, SEILER T. Riboflavin/ultraviolet-a-induced collagen crosslinking for the treatment of keratoconus. **American Journal of Ophthalmology** 2003; 135: 620–627.

MAIER PHILIP., et al. “Corneal Collagen Cross-Linking in the Stabilization of Keratoconus”. **Deutsches Aerzteblatt Online** 116 (2019): 184-190.

MOGHADAM., et al. “The Outcome of Corneal Collagen Cross Linking in Patients with Advanced Progressive Keratoconus: A 2-Year Follow-up Study”. **Middle East African Journal of Ophthalmology** 26.1 (2019): 11.

SPOERL E, HUHLE M, SEILER T. Induction of cross-links in corneal tissues. **Exp Eye Res**. 1998; 66(1):97-103.

SPOERL E, WOLLENSAK G, SEILER T. Increased resistance of cross-linked cornea against enzymatic digestion. **Curr Eye Res**. 2004; 29(1):35-40.

WOLLENSAK G, SPOERL E, WILSCH M et al. Keratocyte apoptosis after corneal collagen cross-linking using riboflavin/UVA treatment. **Cornea** 2004; 23:43–49. Epub 2004/01/01.

TABIBIAN D, RICHOZ O, HAFEZI F. PACK-CXL: corneal cross-linking for treatment of infectious keratitis. **J Ophthalmic Vis Res**. 2015;10: 77–80.

POT SA, GALLHÖFER NS, MATHEIS FL, VOELTER RATSON K,HAFEZI F, SPIESS BM.Cornea lcollagen cross-linking as treatment for infectious and non-infectious corneal melting in cats and dogs: results of aprospective,nonrandomized,controlledtrial. **Vet Ophthalmol**. 2014;17: 250–260.

FAMOSE F. Evaluation of accelerated collagen cross-linking for the treatment of meltingkeratitis in eight dogs. **Vet Ophthalmol**. 2014;17: 358–367.

RAZMJOO., et al. “Cornea Collagen Cross-Linking for Keratoconus: A Comparison between Accelerated and Conventional Methods”. **Advanced Biomedical Research** 6.1 (2017): 10.

FAMOSE. “Evaluation of accelerated corneal collagen cross linking for the treatment of bullous keratopathy in eight dogs”. **Veterinary Ophthalmology** 19.3 (2016: 250-255.

HUANG JINRONG., et al. “Two-Year Topographic and Densitometric Outcomes of Accelerated (45 mW/cm^2) Transepithelial Corneal Cross-Linking for Keratoconus: A Case-Control Study”. **BMC Ophthalmology** 18.1 (2018): 337.

DEMIRBAS NH, PFLUGFELDER SC. Topographic pattern and apex location of keratoconus on elevation topography maps. **Cornea**. 1998; 17:476–84

SHERWIN T, BROOKES NH. Morphological changes in keratoconus: Pathology or pathogenesis. **Clin Exp Ophthalmol**. 2004; 32: 211–7

ALARIO AF, PIRIE CG. Central corneal thickness measurements in normal dogs: a comparison between ultrasound pachymetry and optical coherence tomography. **Vet Ophthalmol**. 2014;17(3):207–211. doi:10.1111/vop.12074 [PubMed: 23763504]

BENTLEY E, MILLER PE, DIEHL KA. Use of high-resolution ultrasound as a diagnostic tool in veterinary ophthalmology. **J Am Vet Med Assoc**. 2003;223(11):1617–1622.doi:10.2460/javma. 2003. 223. 1617 [PubMed: 14664449]

GIBSON TE, ROBERTS SM, SEVERIN GA, STEYN PF, WRIGLEY RH. Comparison of gonioscopy and ultrasound biomicroscopy for evaluating the iridocorneal angle in dogs. **J Am Vet Med Assoc**. 1998;213(5):635–638. [PubMed: 9731256]

RAISKUP-WOLF F, HOYER A, SPOERL E et al. Collagen crosslinking with riboflavin and ultraviolet-A light in keratoconus: long-term results. **Journal of Cataract and Refractive Surgery** 2008; 34: 796 801.

HAFEZI F, KANELLOPOULOS J, WILTFANG R et al. Corneal collagen crosslinking with riboflavin and ultraviolet A to treat induced keratectasia after laser in situ keratomileusis. **Journal of Cataract and Refractive Surgery** 2007; 33: 2035–2040.

HAFEZI F, DEJICA P, MAJO F. Modified corneal collagen crosslinking reduces corneal oedema and diurnal visual fluctuations in Fuchs dystrophy. **British Journal of Ophthalmology** 2010; 94: 660–661. Epub 2010/05/08.

ISELI HP, THIEL MA, HAFEZI F et al. Ultraviolet A/riboflavin corneal cross-linking for infectious keratitis associated with corneal melts. **Cornea** 2008; 27: 590–594

MAKDOUMI K, MORTENSEN J, CRAFOORD S. Infectious keratitis treated with corneal crosslinking. **Cornea** 2010; 29: 1353–1358. Epub 2010/11/26.

SCHRIER A, GREEBEL G, ATTIA H et al. In vitro antimicrobial efficacy of riboflavin and ultraviolet light on Staphylococcus aureus, methicillin-resistant Staphylococcus aureus, and Pseudomonas aeruginosa. **Journal of refractive surgery** 2009; 25: S799–S802. Epub 2009/09/24.

MARTINS SA, COMBS JC, NOGUERA G et al. Antimicrobial efficacy of riboflavin/UVA combination (365 nm) in vitro for bacterial and fungal isolates: a potential new treatment for infectious keratitis. **Investigative Ophthalmology & Visual Science** 2008; 49: 3402–3408. Epub 2008/04/15.

ITO K, INOUE S, YAMAMOTO K et al. 8-Hydroxydeoxyguanosine formation at the 5' site of 5'-GG-3' sequences in double-stranded DNA by UV radiation with riboflavin. **Journal of Biological Chemistry** 1993; 268: 13221 13227. Epub 1993/06/25.

TSUGITA A, OKADA Y, UEHARA K. Photosensitized inactivation of ribonucleic acids in the presence of riboflavin. **Biochimica et Biophysica Acta** 1965; 103: 360–363. Epub 1965/06/08.

ANWAR HM, EL-DANASOURY AM, HASHEM AN. Corneal collagen crosslinking in the treatment of infectious keratitis. **Clinical Ophthalmology** 2011; 5: 1277–1280. Epub 2011/10/04.

HAFEZI F, HOSNY M, SHETTY R, et al. PACK CXL vs. antimicrobial therapy for bacterial, fun gal, and mixed infectious keratitis: A prospective randomized phase 3 trial. **Eye Vis** (Lond). 2022;9 (1):2. Downloaded from tvst.arvojournals.org on 08/28/2023 Modifications of Corneal Cross-Linking Protocols TVST | May2023 | Vol.12 | No.5 | Article18 | 15

KNYAZER B, KRAKAUER Y, TAILAKH MA, et al. Accelerated corneal cross-linking as an adjunct therapy in the management of presumed bacterial kerati tis: A cohort study. **J Refract Surg**. 2020;36(4):258 264.

GALVIS V, TELLO A, ORTIZ, AI, EXCAF LC. Patient selection for corneal collagen cross-linking: an updated review. **Clin Ophthalmol**. 2017; 11:657-668

TANG J, LIU J. Variance of Speed of Sound and Correlation with Acoustic Impedance in Canine Corneas. **Ultrasound Med Biol**. 2011;37(10):1714–1721. doi:10.1016/j.ultrasmedbio.2011.06.012 [PubMed: 21821348]

MARTÍN-SUÁREZ E, GALÁN A, MORGAZ J, GUISADO A, GALLARDO JM, GÓMEZ-VILLAMANDOS RJ. Comparison of central corneal thickness in dogs measured by ultrasound pachymetry and ultrasound biomicroscopy. **Vet J**. 2018; 232:13–14. doi:10.1016/j.tvjl.2017.12.003 [PubMed: 29428083]

JEONG S, KANG S, PARK S, et al. Comparison of corneal thickness measurements using ultrasound pachymetry, ultrasound biomicroscopy, and digital caliper in frozen canine corneas. **Vet Ophthalmol**. 2018;21(4):339–346. doi:10.1111/vop.12509 [PubMed: 29111598]

CHO YW, YOO WS, KIM SJ et al. Efficacy of Systemic Vitamin C Supplementation in Reducing Corneal Opacity Resulting from Infectious Keratitis. **Medicine** 2014; 93(23):e125. doi:10.1097 [PubMed]

VILLABONA-MARTINEZ V, DUTRA BAL et al. Effect of Topical Losartan in the Treatment of Established Corneal Fibrosis in Rabbits. **Translational Vision Science & technology** 2024. 13(8):22. doi:10.1167/tvst.13.8.22

ANNEX 1. PUBLISHED ARTICLE AT VETERINARY OPHTHALMOLOGY IN 2021 TITLED "DEVELOPMENT OF RETINAL BULLAE IN DOGS WITH PROGRESSIVE RETINAL ATROPHY"

Received: 10 June 2021 | Revised: 4 August 2021 | Accepted: 23 August 2021

DOI: 10.1111/vop.12932

ORIGINAL REPORT

WILEY

Development of retinal bullae in dogs with progressive retinal atrophy

Luis Felipe L. P. Marinho[1] | **Laurence M. Occelli**[1] | **Mariza Bortolini**[2] | **Kelian Sun**[1] | **Paige A. Winkler**[1] | **Fabiano Montiani-Ferreira**[2] | **Simon M. Petersen-Jones**[1]

[1]Department of Small Animal Clinical Sciences, College of Veterinary Medicine, Michigan State University, East Lansing, Michigan, USA

[2]Department of Veterinary Medicine, Federal University of Paraná, Curitiba, PR, Brazil

Correspondence
Fabiano Montiani-Ferreira, Department of Veterinary Medicine, Federal University of Paraná, Rua dos Funcionários 1540, 80035–050 Curitiba, PR, Brazil.
Email: montiani@ufpr.br

Simon M. Petersen-Jones, Dept. of Small Animal Clinical Sciences, College of Veterinary Medicine, Michigan State University, 736 Wilson Road, D-208, East Lansing, MI 48824, USA.
Email: Peter315@msu.edu

Funding information
Myers-Dunlap Endowment for canine health, MSU/Universidade do Parana/ fundings, NIH R24EY027285.

Abstract

Objective: To report the development of focal bullous retinal detachments (bullae) in dogs with different forms of progressive retinal atrophy (PRA).

Procedures: Dogs with three distinct forms of PRA (PRA-affected Whippets, German Spitzes and *CNGB1*-mutant Papillon crosses) were examined by indirect ophthalmoscopy and spectral domain optical coherence tomography (SD-OCT). Retinal bullae were monitored over time. One *CNGB1*-mutant dog was treated with gene augmentation therapy. The canine *BEST1* gene coding region and flanking intronic sequence was sequenced in at least one affected dog of each breed.

Results: Multiple focal bullous retinal detachments (bullae) were identified in PRA-affected dogs of all three types. They developed in 4 of 5 PRA-affected Whippets, 3 of 8 PRA-affected Germans Spitzes and 15 of 20 *CNGB1*-mutant dogs. The bullae appeared prior to marked retinal degeneration and became less apparent as retinal degeneration progressed. Bullae were not seen in any heterozygous animals of any of the types of PRA. Screening of the coding region and flanking intronic regions of the canine *BEST1* gene failed to reveal any associated pathogenic variants. Retinal gene augmentation therapy in one of the *CNGB1*-mutant dogs appeared to prevent formation of bullae.

Conclusions: Retinal bullae were identified in dogs with three distinct forms of progressive retinal atrophy. The lesions develop prior to retinal thinning. This clinical change should be monitored for in dogs with PRA.

KEYWORDS

BEST1, bullae, bullous retinal detachment, *CNGB1*, dog, progressive retinal atrophy

Marinho and Occelli contributed equally.

How to cite this article: Marinho LFLP, Occelli LM, Bortolini M, et al. Development of retinal bullae in dogs with progressive retinal atrophy. Vet Ophthalmol. 2022;25: 109– 117. https://doi.org/10.1111/vop.12932